EG&G Idaho, Inc.   (LTR)   Report No. **LO-14-81-074**

Date: **June 16, 1981**

RELEASED BY LOFT CDCS

NRC Research and Technical Assistance Report

USNRC-P394

INTERNAL TECHNICAL REPORT

Title   NUCLEAR FUEL ROD SIMULATION USING
ELECTRICAL HEATER RODS

Organization: LOFT Instrumented Fuels Branch

RECEIVED
JUL 14 1981
U.S. NUCLEAR REGULATORY
COMMISSION

Author: _____M. L. Carboneau_____

NRC Research and Technical
Assistance Report

Checked By: _____M. L. Russell_____   Approved By: _____D. J. Hanson_____

LOFT TECHNICAL REPORT

Title NUCLEAR FUEL ROD SIMULATION USING ELECTRICAL HEATER RODS	LTR No. LO-14-81-074
Author Michael L. Carboneau *M L Carboneau*	Released By LOFT CDCS
Performing Organization LOFT Instrumented Fuels Branch FES Supv.	Date June 16, 1981
	Pro, ct System Engineer
LOFT Review and Approval	*M. L. Russell*
RSB Mgr. LMD Mgr.	IFB Mgr.

The purpose of this report is to examine the theory and simulation capabilities of selected sheath-heated and internally-heated electrical rods for reproducing nuclear rod behavior. In the process of examining the Semiscale MOD-1 heater rod, an algorithm is developed for computing the input power function needed to force the MOD-1 rod to duplicate the LOFT L2-3 nuclear rod data. It is observed that in order for the Semiscale rod to simulate the L2-3 measured data, large quantities of negative power must be supplied to the rod prior to and during rod quench. This indicates that it is not possible for the MOD-1 heater rod to exactly duplicate the rapid cooling phenomenon observed for the LOFT nuclear rods during the L2-3 test.

DISPOSITION OF RECOMMENDATIONS

No disposition required.

NRC Research and Technical Assistance Report

ABSTRACT

The theory, simulation capabilities, and limitations of direct and indirect heated electrical rods to reproduce nuclear rod behavior during rapid cooling events are examined. In particular, calculations are made of the local rod power function for the Semiscale Mod-1 heater rod needed to force this rod to reproduce the measured cladding quench data from the LOFT L2-3 experiment. Finally, suggestions for improving the simulation capabilities of current electric rod designs are presented.

NRC Research and Technical
Assistance Report

SUMMARY

This report examines the capabilities and limitations associated with simulating nuclear rod behavior with some currently designed surface heated and internally heated electric rods. The theory of the Zaloudek and LOBI (Loop Blowdown Investigation Facility)* direct heater rods, as well as the Semiscale solid type indirect heater rod are reviewed.

For the Semiscale (solid type) heater rod an alogrithm is developed for evaluating the local rod power needed to force the rod to duplicate two prescribed surface boundary conditions. The principal result of the calculations and supporting analyses indicates that in order for the Semiscale heater rod to reproduce the LOFT L2-3 nuclear rod temperature quench data, unrealistic negative rod powers are needed to compensate for the high internal thermal conductivity of the rod (BN vs. UO_2), which causes the stored energy in the Semiscale heater rod to be transferred to the cladding surface more rapidly than normally occurs in a nuclear rod. This characteristic of the Semiscale rod and other indirect heater rods, results in an inherent design limitation for simulating rapid cooling events.

In comparison to the solid type (indirect) heater rods, some of the sheath heated (or directly heated) rods have a distinct advantage. For instance, from theoretical calculations it can be shown that the Zaloudek type heater rod can be realistically powered in such a manner as to afford perfect simulation under all possible nuclear rod events. However, the assumptions made in order to derive this result are somewhat unrealistic when applied to a real rod. Furthermore, as in the case for solid type

NRC Research and Technical Assistance Report

---

* All acronyms used in the report are defined in Appendix C.

internally heated rods, the nuclear rod surface boundary conditions must be known in order to calculate the proper rod power function for the Zaloudek rod.

It appears that the LOBI heater rod might also be able to reproduce nuclear rod behavior, but since the response of the rod is extremely sensitive to the driving power function, it's difficult to utilize the LOBI rod to predict unknown nuclear rod phenomena. Instead, the LOBI rod is generally used for only code verification studies.

The ideal fuel rod simulator would "naturally" respond like a nuclear rod under a broad range of test conditions with little or no input rod power. This is desirable since the electric rod power function is dependent upon nuclear rod boundary conditions that are usually not well known, or in some cases, totally unexpected prior to testing. This occurred when the Semiscale counter part tests failed to indicate the LOFT L2 nuclear rod rewet events. It is now known that the Semiscale heater rod has difficulties in simulating such events.

NRC Research and Technical
↘ Assistance Report

CONTENTS

FIGURES

NRC Research and Technical
Assistance Report

APPENDIX A FIGURES

APPENDIX B FIGURES

NUCLEAR FUEL ROD SIMULATION USING ELECTRICAL HEATER RODS

1. OBJECTIVES

The purpose of this study is to investigate the basic theory associated with electrical rod simulation of nuclear rod behavior, and then use this information to illustrate the inherent difficulties that many heater rod designs have in simulating rapid cooling transients. Also, identification of some key design criteria will be made in order to facilitate future heater rod designs that better simulate or typify nuclear fuel rod behavior during loss-of-coolant experiments (LOCEs). Finally, it will be demonstrated that the Semiscale heater rod cannot reproduce the nuclear rod cooldown behavior observed during the LOFT L2-3 test, unless the rod is powered according to an unrealistic negative rod power function.

2. INTRODUCTION

A major problem that is addressed in the report is the determination
of a method or algorithm by which a time dependent heat source distribution
$[q_E'''(r,t)]$ can be evaluated for a given electric rod design so that the
electric rod will simulate the behavior of a nuclear rod. As we shall see,
however, the electric rod heat source distribution generally depends upon
the surface temperature and heat flux response of the nuclear rod during
the experiment. This means that, in general, it is not possible to power
an electric rod with one and only one sort of "decay power" function and
expect the electric rod to exactly duplicate the response of the nuclear
rod in every possible transient, even though the hydraulic boundary
conditions agree. Furthermore, the power input to the electric rod depends
upon the nuclear rod boundary conditions. In other words, most electric
rod designs must be powered according to formulas which themselves depend
upon a prior knowledge of, or at least an expectation of, the response of
the nuclear rod in the postulated transient.

Although the response of a nuclear rod to a particular thermal-
hydraulic transient is usually not known, a "target" response might be
postulated and then an appropriate electric rod power could then be
calculated. If the response of the electric rod is not very sensitive to
the input power, then the actual response of the electric rod might be
reasonably close to that of the nuclear rod response even though the
"targeted" curve is not exactly correct. The difference between a
mathematically exact duplication and a reasonably close approximation is
rather large. It is not known at this time how close of an approximation
is close enough in order to adequately simulate the required thermal-
hydraulic boundary conditions.

It may turn out that an electrical rod that has the theoretical capability of simulating a nuclear rod will not function as expected under experimental conditions, and that another electric rod design which according to theory cannot exactly duplicate a nuclear rod response may indeed provide better simulation, and would therefore represent a better design.

Resolution of these problems can only be achieved by both computer analysis and experimental testing. The interaction between the various rod parameters defined by rod geometry, materials, location and powering of heater elements are far too complex to analyze in one all encompassing theory. Instead, it is the objective of the report to develop some basic theory concerning electric rod simulation of nuclear rods, and then use this information to provide some guidance and insight into developing better electric rod designs, and suggest reasons that explain why some heater rods may not be as good as others. Also, some formulas will be derived showing the relationship between electric rod input power and the nuclear rod boundary conditions.

3. BOUNDARY CONDITIONS

We begin by defining the term "simulation." An electric rod is said to simulate the response of a nuclear rod (or vise versa) if the surface heat flux and the surface temperature of both rods are respectively equal during the given experiment. These two conditions necessarily imply that the heat transfer coefficient of both rods will be the same as long as the bulk coolant temperatures are equal. Consequently, if these conditions are satisfied, then the heat transfered between the rod and coolant will be the same for both the electric and nuclear rods.

In symbols, electric-nuclear rod simulation means that Equations (1a) and (1b) are valid.

Identical surface heat fluxes:

$$\phi_E \Big|_{surface} = \phi_N \Big|_{surface} \tag{1a}$$

Identical surface temperatures:

$$T_E \Big|_{surface} = T_N \Big|_{surface} \tag{1b}$$

In cylindrical coordinates with no axial heat conduction and azimuthal symmetry, the electric and nuclear heat fluxes are defined by Equations (2a) and (2b), respectively.

$$\phi_E = - k_E \frac{\partial T_E}{\partial r} \tag{2a}$$

$$\phi_N = - k_N \frac{\partial T_N}{\partial r} \tag{2b}$$

Here, $T_E = T_E(r,t)$ and $T_N = T_N(r,t)$ are the electric and nuclear rod space-time temperature distributions. The respective material thermal conductivities are k_E and k_N. That is, $k_E = k_E(T_E)$ and $k_N = k_N(T_N)$.

4. ONE DIMENSIONAL HEAT CONDUCTION

We begin with the one-dimensional heat conduction equation written in vector notation:[1]

$$\nabla \cdot k \nabla T - \rho C_p \frac{\partial T}{\partial t} = -q'''(\bar{r},t) \tag{3a}$$

where

$$T = T(\bar{r},t) \tag{3b}$$

$$k = k(T) \tag{3c}$$

$$\rho C_p = \rho(T)C_p(T) \tag{3d}$$

Here, $T(\bar{r},t)$ is the local temperature of the solid, $\rho(T)$ and $C_p(T)$ are the density and specific heat, respectively, $k(T)$ is the thermal conductivity, and $q'''(\bar{r},t)$ is the volumetric heat generation term. Also, the vector $\bar{r} = x\hat{i} + y\hat{j} + z\hat{k}$.

For cylindrical rod geometry with azimuthal symmetry and no axial heat conduction, system (3) can be written in the following form:

$$\frac{1}{r} \frac{\partial}{\partial r} \left(r \, k \, \frac{\partial T}{\partial r} \right) - \gamma \frac{\partial T}{\partial t} = -q'''(r,t) \tag{4a}$$

where

$$T = T(r,t) \tag{4b}$$

$$k = k(T) \tag{4c}$$

$$\gamma = \rho C_p = \rho(T) \, C_p(T) \tag{4d}$$

6

For simplicity, the symbol $\gamma = \rho C_p$ has been introduced to represent the volumetric specific heat. Consequently, thermal diffusivity can be written as: $\alpha = k/\gamma$.

Notice that in cylindrical geometry with azimuthal symmetry and only radial heat conduction, the gradient and divergence operators have been interpreted as follows:

$$\text{grad } (T) = \nabla T = \frac{\partial T}{\partial r} \hat{e}_r \tag{5a}$$

$$\text{div } (V(r) \, \hat{e}_r) = \nabla \cdot (V(r) \, \hat{e}_r) = \frac{1}{r} \frac{\partial}{\partial r} [r \, V(r)] \tag{5b}$$

Where e_r is a unit vector in the "+r" direction, e.g. $\hat{e}_r = (x\hat{i} + y\hat{j} + z\hat{k})/\text{SQR}(x^2 + y^2 + z^2)$. Notice Figure 1.

INEL-A-17 564
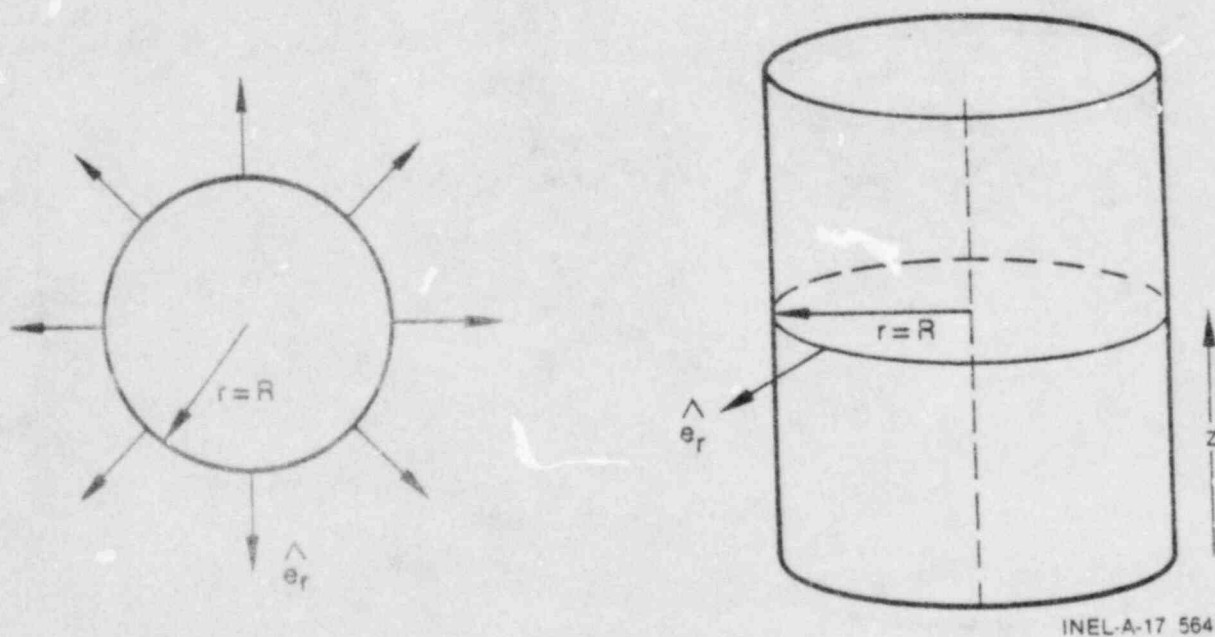
Fig. 1. Rod geometry showing the cylinder radius ($r = R$) and unit vectors $\hat{e}_r$ normal to the surface of the cylinder.

7

Since k and $\gamma = \rho C_p$ are generally functions of temperature, T, the differential Equations (3a) or (4a) will not be linear in T. Since it is very difficult to solve non-linear partial differential equations, we shall assume that k and $\gamma = \rho C_p$ are not directly dependent on temperature. For example, given a space-time temperature distribution $T = T(r,t)$, then $k = k(T)$ and $\gamma = \gamma(T)$; and therefore,

$$k = k[T(r,t)] \tag{6a}$$

and,

$$\gamma = \gamma[T(r,t)] \tag{6b}$$

Consequently, if T is a known function of r and t, then k and γ will be functions of r and t. From Equations (6a) and (6b), k and γ are therefore functions of the variables r and t; however, r and t are not completely independent since they are related via the T function. In general, the solution temperature $T(r,t)$ is not known so that k and γ are not known as functions of r and t. Nevertheless, if one assumes that some initial estimate can be made for T, say $T_0(r,t)$, then an estimate can be made for k and γ based on T_0 as follows:

$$k_0 = k_0(r,t) \equiv k[T_0(r,t)] \tag{7a}$$

$$\gamma_0 = \gamma_0(r,t) \equiv \gamma[T_0(r,t)] \tag{7b}$$

Since k_0 and γ_0 are written as only functions of r and t, and not T, then Equation (4a) is linear in T. Solving the modified linear differential equation (with estimates made for k and γ), one obtains a new estimate for T, say T_1. Next, using k_1 and γ_1 based on T_1 in Equation (4a), another new estimate for T, say T_2, can be made. Hopefully, by going through enough iterations one can obtain a sequence of functions: $<k_i>$, $<\gamma_i>$, and $<T_i>$ such that:

$$T(r,t) = \lim_{i \to \infty} T_i(r,t)$$

$$k[T(r,t)] = \lim_{i \to \infty} k_i(r,t)$$

$$\gamma[T(r,t)] = \lim_{i \to \infty} \gamma_i(r,t)$$

In this way one can attempt to solve a non-linear partial differential equation by solving a sequence of linear partial differential equations, each of which are easier to solve than the original problem.

Although no attempt will be made in the report to actually carry out the procedure described above, a justification has been made for assuming that k and γ can be treated as functions of r and t only. Throughout the report we shall assume that estimates can be made for k and γ in terms of the independent variables r and t. For instance,

$$k = k(r,t) \tag{8a}$$

$$\gamma = \gamma(r,...) \tag{8b}$$

Special cases of Equations (8) occur when k and γ are either constants throughout the rod, or when they are simply functions of r only. In fact, for much of the analysis that follows we shall assume that the rod thermal properties do not change very much, and therefore, reasonable estimates can be made for k and γ in terms of the variable r only. In this case we would write:

$$k = k(r) \tag{9a}$$

$$\gamma = \gamma(r) \tag{9b}$$

5. INTRODUCTORY THEORY

To begin, let $k_E = k_E(r,t)$ and $\gamma_E = \gamma_E(r,t)$ represent
functions of the thermal conductivity and volumetric specific heat
of the materials comprising the electric rod design; and $k_N = k_N(r,t)$
and $\gamma_N = \gamma_N(r,t)$ be the respective values for the nuclear rod.
Also, let $T_E = T_E(r,t)$ and $T_N = T_N(r,t)$ represent the space-time
temperature distributions in the electric and nuclear rods. Likewise,
the heat fluxes for the electric and nuclear rods are respectively:

$$\phi_E = \phi_E(r,t) = -k_E \left.\frac{\partial T_E}{\partial r}\right|_{r,t} \tag{10a}$$

and

$$\phi_N = \phi_N(r,t) = -k_N \left.\frac{\partial T_N}{\partial r}\right|_{r,t} \tag{10b}$$

To simplify writing of the heat conduction differential Equation (4a),
we introduce the operators D_E and D_N defined as follows:

$$D_E(T) \equiv \frac{1}{r}\frac{\partial}{\partial r}\left(r k_E \frac{\partial T}{\partial r}\right) - \gamma_E \frac{\partial T}{\partial t} \tag{11a}$$

and for the nuclear rod:

$$D_N(T) \equiv \frac{1}{r}\frac{\partial}{\partial r}\left(r k_N \frac{\partial T}{\partial r}\right) - \gamma_N \frac{\partial T}{\partial t} \tag{11b}$$

Using the notation we have developed, the heat conduction differential
equation for the electric rod with solution temperature distribution T_E
is:

10

$$D_E(T_E) = - q_E'''(r,t) \tag{12}$$

Here, $q_E'''(r,t)$ is the power density source term. A similar equation could be written for the nuclear rod.

5.1 Simulation Criteria

In order to simulate a nuclear rod with an electric rod two important boundary conditions must be satisfied simultaneously. Namely, the surface temperatures and surface heat fluxes of the electric and nuclear rods must agree. In symbols:

$$T_E(R,t) = T_N(R,t) \tag{13a}$$

$$\phi_E(R,t) = \phi_N(R,t) \tag{13b}$$

Here, $r = R$ defines a boundary surface of the rods (both rods are assumed to have the same outside radius OR) where the two respective boundary conditions are to agree. In general, $r = R$ will represent the outer surface of rods, however, a different inner cylindrical surface could also be selected, e.g., the inside cladding surface or fuel pellet surface.

The difficult aspect of fuel rod simulation requires that one find a power source term $q_E'''(r,t)$ for the electric rod so that both T_E and ϕ_E agree with T_N and ϕ_N, respectively at $r = R$ and for all times t. That is, find a function $q_E'''(r,t)$ such that the solution of Equation (12) satisfies the two boundary conditions (13a) and (13b).

The uniqueness theorem for the heat conduction differential equation (proved in References 2 and 3) stipulates that for any prescribed function $q_E'''(r,t)$ and a boundary condition for either T_E or ϕ_E, and some prescribed initial temperature distribution $[T_E(r,0)]$, there is at most

11

solution to the differential equation: $D_E(T) = -q_E'''$. Also, for
the same boundary and initial conditions, existence theorems for partial
differential equations show that there is a solution for the given
problem.[3]

The problem at hand is that there is no guarantee that one can
find a source term $q_E'''(r,t)$ such that $T = T_E$ solves the differential
Equation (12) subject to two boundary conditions. Indeed, if the electric
rod design is such that the r dependency in $q_E'''(r,t)$ is already specified
by the particular design and positioning of the heater rod element(s),
e.g., $q_E'''(r,t) = P(r) Q(t)$ where $P(r)$ is determined by rod design, then
there may be no function $Q(t)$ which solves the problem. At the other end
of the spectrum, if one were willing to admit any real functions $q_E'''(r,t)$
where q_E may not even be a separable function of the variables r and t,
then there will be an infinite number of solutions. However, many of these
solutions will not be realistically possible since the source functions
take on negative values for some values of r and t.

We begin our study of the simulation capabilities of electrical heater
rods by first examining sheath heated (direct heated) rods and then later
considering internally heated (indirect heated) electric rods.

6. SURFACE HEATED ELECTRICAL RODS

A direct heater rod usually consists of a metallic sheath surrounding a ceramic insulator. The insulator material is sometimes selected so that its thermal properties a e similar to that of nuclear fuel (UO_2). Heat is generated in a direct ﹍ ﹍ ter rod by passing an electric current directly through the outer sheath or cladding of the rod, which eliminates the need for a heater filament inside the insulator. Figure 2 depicts the basic features associated with a surface heated electric rod. Notice from the figure that the cladding thickness of the rod is varied so that a sinusoidal axial power distribution is formed.

A method published by F. R. Zaloudek, and summarized in Reference 4, illustrates a power scheme by which one particular type of direct heater rod can be powered so that simulation of a nuclear fuel rod is theoretically possible. The method relies upon the following criteria:

1. The dimensions, thermal conductivity, volumetric specific heat, and gap resistance of the electric and nuclear rod are equivalent.

2. The energy deposited in the cladding of the rod can be assumed to appear as a boundary surface heat source.

3.* The thermal properties of the electric rod are assumed to be independent of temperature. (This is assumed so that the resultant differential equation is linear in T.)

---

* It is possible that Criteria 3 may be relaxed somewhat by considering the solution of the non-linear temperature dependent heat conduction differential equation as a limiting sequence of solutions to temperature independent linear differential equations as shown in Section 4.

Cladding

Ceramic
insulation

Gap

Centerline hole

Thermocouple

Cladding with
variable wall
thickness

Ceramic
insulation

Centerline hole

Gap

INEL-A-17 557
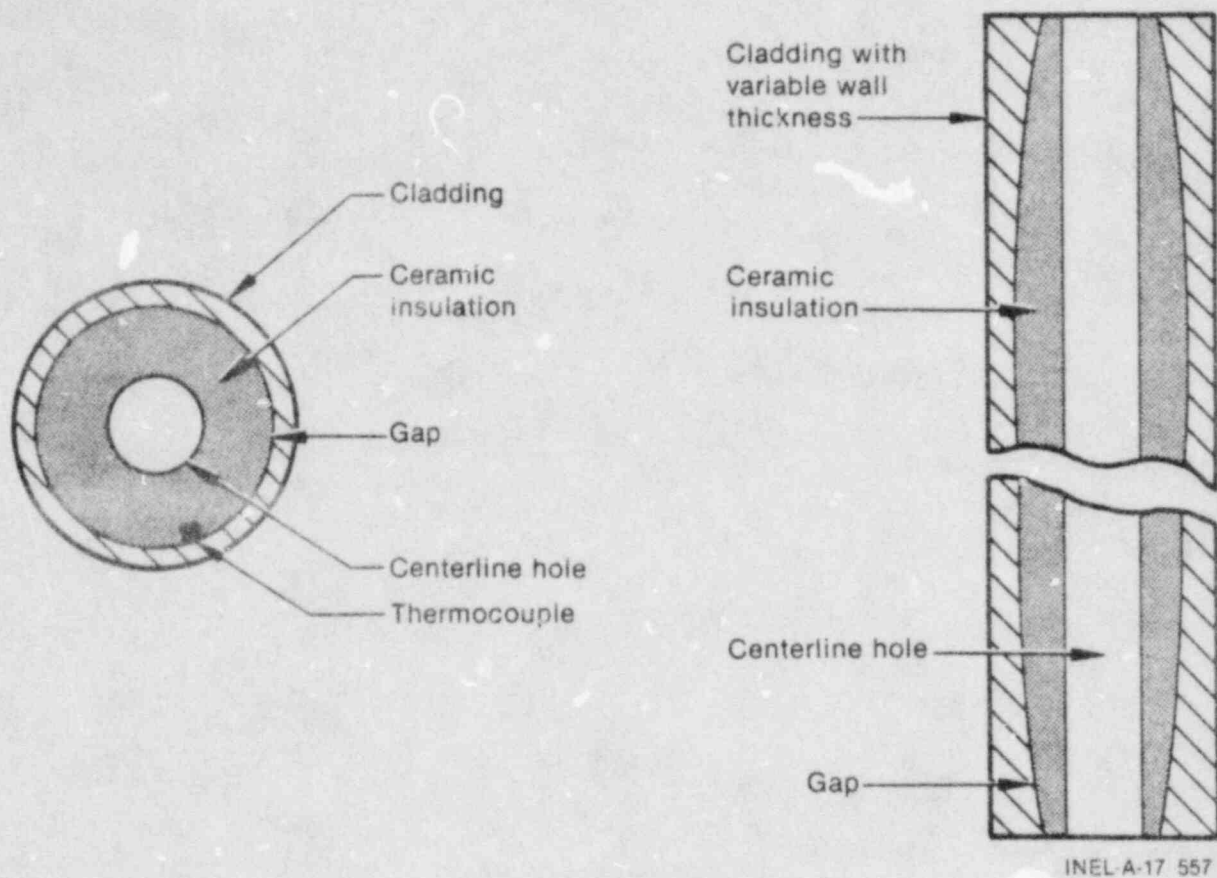
Fig. 2. An example of a direct heater rod with variable cladding
thickness, and a ceramic filler material that helps to
simulate rod stored energy. Some direct heater rods, like
the LOBI rod, do not have this insulation material. In the
Zaloudek heater rod, the insulation material is UO_2 and the
cladding is zircaloy.

Although the above criteria can not be exactly met, experience with sheath heated rods has shown that good simulation is possible with some rod designs that are less than ideal.

We now demonstrate how it is possible to power a sheath heater rod, that conforms with Criteria 1, 2, and 3, and yield a rod surface temperature and surface heat flux that duplicates the corresponding boundary conditions of a nuclear rod. The procedure developed here parallels the method developed by Zaloudek.

6.1 Theory of the Zaloudek Heater Rod

To begin let $T_E = T_E(r,t)$ represent the electric rod space-time temperature, and define the function $T_e(r,t)$ by Equation (14).

$$T_e(r,t) \equiv T_N(r,t) - U(r,t) + U(R,t) \tag{14}$$

Where $T_N(r,t)$ is the space-time temperature distribution in the nuclear rod, and $U(r,t)$ is a temperature function satisfying the following equations:

$$(DE)^* \quad D_N(U) = -q_N'''(r,t) \tag{15a}$$

$$(BC)^* \quad U(R,t) = \text{a constant } U(R,0) \tag{15b}$$

Well cooled nuclear rod model

$$(IC)^* \quad U(r,0) = -T_E(r,0) + T_N(r,0) + U(R,0) \tag{15c}$$

---

* DE = differential equation, BC = boundary condition, and IC = initial condition.

Here, $T_E(r,0)$ represents the electric rod initial temperature distribution, $T_N(r,0)$ the nuclear rod initial temperature distribution, and $U(R,0)$ some arbitrary positive constant. A value for $U(R,0)$ is selected in order to avoid negative temperature solutions for $U(r,t)$ in system (15). We will eventually prove that $T_e = T_E$.

The D_N operator in (15) is based on materials with thermal properties k_N and γ_N; however, since $k_N = k_E$ and $\gamma_N = \gamma_E$ (Criteria 1), then the operators D_N and D_E are equivalent. Also, since k_E and γ_E are independent of temperature (Criteria 3), then k_N and γ_N are temperature independent and therefore the operator D_N is linear. Finally, $q_N'''(r,t)$ is the nuclear rod power density distribution.

The differential Equation (15a), boundary condition (15b), and initial condition (15c) taken together describe a system which is usually referred to as a "well cooled" rod. The term "well cooled" refers to the fact that the surface temperature $[U(R,t)]$ does not change, although the stored energy and heat generation in the rod may change with time. Clearly, for a "well cooled" rod all of the energy generated inside the rod must be transported to the coolant without affecting the surface cladding temperature.

It may be surprising, but nevertheless true, that the solution of system (15) provides a means by which the surface heat source for the above designed direct heater rod can be determined. We proceed as follows:

First, solve system (15) and determine the function $U(r,t)$. This is most efficiently accomplished by running a heat conduction code subject to the specified boundary and initial conditions. Next, compute the gradient of T_e from Equation (14) and then evaluate $-k_N \nabla T_e$. Doing this we find that:

$$\nabla T_e \Big|_{r,t} = \nabla T_N \Big|_{r,t} - \nabla U \Big|_{r,t} + 0 \qquad \text{for } r < R \tag{16a}$$

$$-k_E \left. \nabla T_e \right|_{r,t} = -k_N \left. \nabla T_e \right|_{r,t} = -k_N \left. \nabla T_N \right|_{r,t} + k_N \left. \nabla U \right|_{r,t} \qquad \text{for } r < R \qquad (16b)$$

$$-k_E \left. \nabla T_e \right|_{R,t} = -k_N \left. \nabla T_e \right|_{R,t} = -k_N \left. \nabla T_N \right|_{R,t} + k_N \left. \nabla U \right|_{R,t} + S_E(R,t) \quad \text{for } r=R \quad (16c)$$

Here $S_E(R,t)$ is the electric rod surface heat source term (W/cm^2) and is included in Equation (16c) because the energy source for the direct heater rod is treated as a surface boundary condition (Criteria 2), and not part of the differential equation. Defining $\phi_E = -k_E \Delta T_e$, then Equation (17) directly follows from (16c):

$$\underbrace{\phi_E(R,t)}_{\substack{\text{electric} \\ \text{surface} \\ \text{heat flux}}} = \underbrace{\phi_N(R,t)}_{\substack{\text{nuclear} \\ \text{surface} \\ \text{heat flux}}} - \underbrace{\left(-k_N \left. \nabla U \right|_{R,t} \right)}_{\substack{\text{the well cooled} \\ \text{rod surface} \\ \text{heat flux}}} + \underbrace{S_E(R,t)}_{\substack{\text{electric} \\ \text{rod surface} \\ \text{heat source}}} \qquad (17)$$

Since we want the surface heat flux on the electric and nuclear rod to agree, i.e., $\phi_E(R,t) = \phi_N(R,t)$, then we must select the surface heat source term $S_E(R,t)$ to be equal to the heat flux that is emitted from the surface of the well cooled nuclear rod. In symbols,

$$S_E(R,t) \equiv -k_N \left. \nabla U \right|_{R,t} \qquad (18)$$

Therefore, Equation (17) reduces to:

$$\phi_E(R,t) = \phi_N(R,t) + 0 \qquad (19)$$

Notice that since $q_N'''(r,t) \geq 0$ and $U(R,0)$ is a constant, then the well cooled nuclear rod will always have a non-negative surface heat flux, which means that the electric rod surface heat source term is also non-negative.

Finally, all that remains to be proved is that the function $T_e(r,t)$, as determined by the above equations is the required solution of the electric rod heat conduction equation described in Equations (20a) thru (20d):

Direct Heater Rod Equations

(DE) $D_E(T_E) = 0$ (no internal heat source)   (20a)

(BC1) $T_E(R,t) = T_N(R,t)$ (for all t)   (20b)

(BC2) $\phi_E(R,t) = \phi_N(R,t)$ (for all t)   (20c)

(IC) $T_E(r,0) =$ some initial temperature distribution   (20d)

To verify that $T_e = T_E$, it is only necessary to verify that T_e, as defined by Equation (14), satisfies the conditions specified in Equations (20a) through (20d). This occurs, because there is at most one solution for the above system of equations. Therefore, if T_e satisfies the above equations it must be the one and only one solution.

First, recall that since $k_E = k_N$ and $\gamma_E = \gamma_N$, then $D_E = D_N$. Therefore, operating on both sides of Equation (14) we find that:

$$D_E(T_e) = D_N(T_e) = D_N(T_N) - D_N(U) + D_N[U(R,t)]$$ (21)

Since $D_N(T_N) = -q_N'''$, $D_N(U) = -q_N'''$, and $D_N[U(R,t)] = D_N[U(R,0)] = 0$, then $D_N(T_e) = -q_N''' + q_N''' + 0 = 0$. Hence Equation (20a) is satisfied.

Also, direct substitution of $r = R$ in Equation (14) will show that $T_e(r,t) = T_N(R,t)$. Notice that it has been tacitly assumed that the surface heat source does not affect the rod surface temperature but only corrects for the heat flux delivered to the coolant.

Next, by the judicious selection of $S_E(R,t)$ [note Equation (18)], we have shown that $\phi_E(R,t) = \phi_N(R,t)$ [Equation (19)]. Finally, the initial temperature condition is satisfied since $T_e(r,0) = T_N(r,0) - U(r,0)* + U(R,0) = T_N(r,0) + T_E(r,0) - T_N(r,0) - U(R,0) + U(R,0) = T_E(r,0)$.

Therefore, $T_e(r,t)$ is the electric rod temperature function which satisfies the electric rod heat conduction Equation (20a) subject to the two simultaneous nuclear boundary conditions (20b) and (20c). Therefore, it is possible to power a Zaloudek type sheath heated rod, with a non-negative surface heat source, and duplicate the surface response of a nuclear rod.

6.2 Theory of a LOBI Type Heater Rod

The LOBI (Loop Blowdown Investigations) test facility is located at Ispra in northern Italy and is operated as a joint European research program.[5] The primary purpose of the facility is to provide experimental data for the assessment of computer codes for blowdown type experiments.

In the LOBI facility, nuclear fuel rods are simulated by electrically heated hollow type (stainless steel) tubes. Figure 3 compares the cross sections of a nuclear fuel rod and a LOBI heater rod. To produce a chopped cosine axial power profile, the LOBI rod is designed with five different axial regions of varying tube thickness.

---

* Notice how $U(r,0)$ was selected in Equation (15c).

Nuclear fuel rod
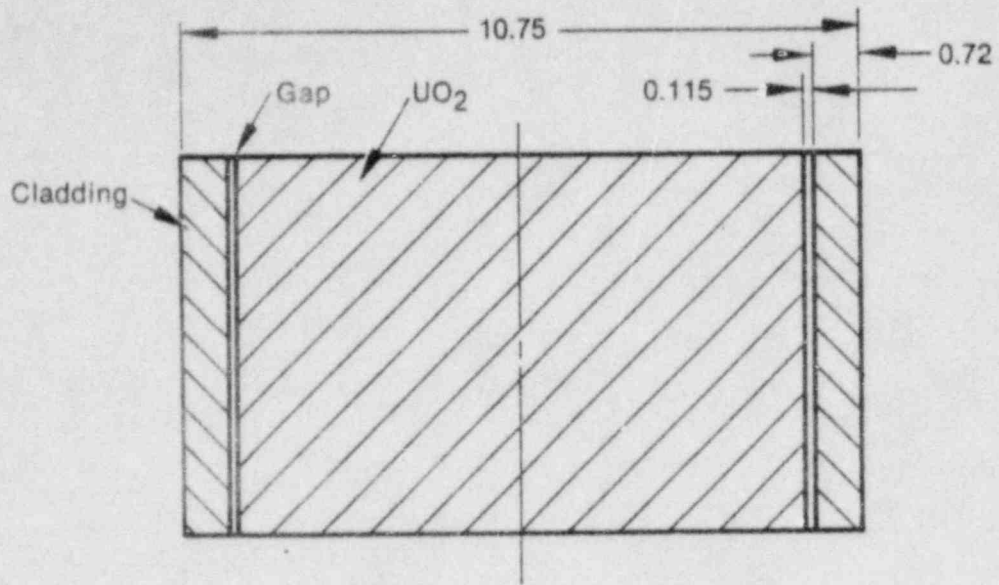
LOBI heater rod, middle section
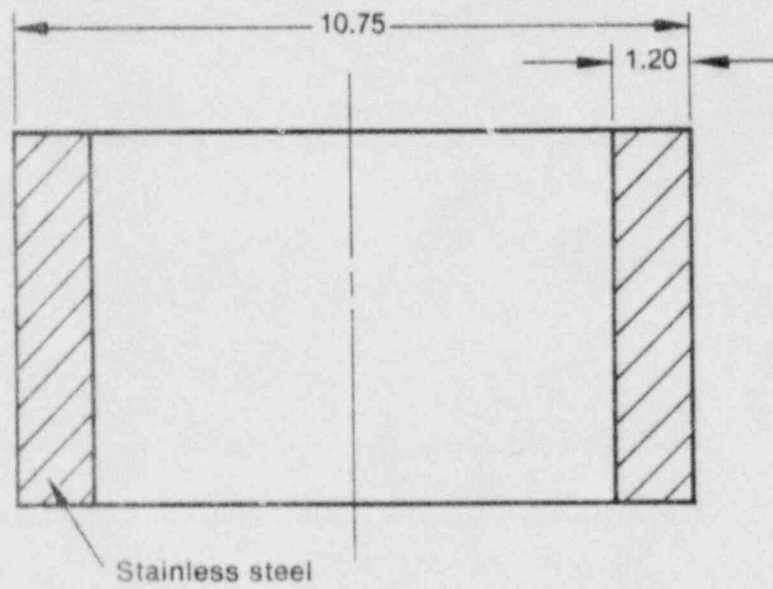
(all measurements in mm)

INEL-A-17 750

Fig. 3. A cross section of a nuclear fuel rod and a LOBI heater rod.

Due to the design and material differences between a nuclear and LOBI
heater rod, the LOBI rod response will normally be different than the
nuclear rod unless the LOBI rod is powered in such a way as to compensate
for the lack of stored energy. However, as will be demonstrated, the
required power function necessary to duplicate the response of a nuclear
rod is itself a function of the nuclear surface boundary conditions, which
are usually not well known. Because of the rod design, the LOBI rod cannot
be successfully used to estimate the unknown response of a nuclear rod
during an unpredictable hydraulic event. This occurs because the LOBI rod
response is greatly affected by the rod input power function, and the
correct power function is itself a function of the very same nuclear
boundary conditions that we are attempting to measure.

The following equation illustrates the functional relationship
between the correct LOBI power function [$q'''(t)$] and the nuclear surface
boundary conditions: $T_N(R,t)$ and $\phi_N(R,t)$. Derivation of the formula
is obtained by a straight forward Taylor series approximation to the
electric rod temperature function $T(r,t)$ which solves the heat conduction
differential equation in the LOBI rod. The details of the solution are
presented in Reference 5.

For the LOBI heater rod, the required power density function needed to
reproduce the nuclear rod surface conditions is:

$$q'''(t) = \left[\frac{2 R_o}{R_o^2 - R_i^2} \right] \phi_N(R,t) + \gamma \frac{\partial T_N(R,t)}{\partial t}$$

$$+ \left[\frac{(R_o - R_i) R_o}{3R_o - R_i} \right] \frac{1}{\alpha} \left[\frac{\partial \phi_N(R,t)}{\partial t} \right] \tag{22}$$

where

γ $\quad=\quad$ the volumetric heat capacity of stainless steel

α $\quad=\quad$ k/γ the thermal diffusivity of stainless steel

$R = R_o$ $\quad=\quad$ the outer radius of the rod

R_i $\quad=\quad$ the inner radius of the rod

t $\quad=\quad$ time

$T_N(R,t)$ $\quad=\quad$ the nuclear rod surface temperature

$\phi_N(R,t)$ $\quad=\quad$ the nuclear rod surface heat flux

$q'''(t)$ $\quad=\quad$ the volumetric heat generation rate

Equation (22) is reasonably valid if the wall thickness, which is the heater element, is not very large. As is evident from Equation (22), the required power function $q'''(t)$ is directly related to the time dependent boundary functions $T_N(R,t)$ and $\phi_N(R,t)$. All other terms in Equation (22) are constant.

For the LOBI rod two major problems exist in simulating nuclear rod behavior. First, it is important to accurately predict the nuclear rod surface boundary conditions in order to calculate the correct electric rod power function. And second, it is important to make sure that the nucle and electric rod hydraulic conditions agree. That is, utilization of the correct rod power function will not necessarily ensure that the electric rod surface response will duplicate the nuclear rod surface response when the hydraulic conditions are different. Both the correct rod power and the same hydraulic conditions must exist before proper simulation of a nuclear rod can occur.

7. SIMULATION CAPABILITIES OF SOLID TYPE INTERNALLY HEATED ELECTRIC RODS

Unlike the surface heated rods already discussed, internally heated or indirect heater rods generate power in heater elements that are embedded inside the rod and separated from the rod cladding by an insulation barrier. Figures 4, 5, and 6 show examples of solid type and cartridge type internally heated electric rods. A solid type rod is distinguished from a cartridge type rod, and a nuclear rod, by the absence of a gap or gas annulus between the cladding and the inner heat source. Consequently, the cladding of a solid type heater rod can usually be considered as directly coupled to the inner rod stored energy and heat source via a relatively low thermal resistance path provided by the thermal insulation. In contrast, the cladding response of a cartridge type electric rod, or nuclear rod, is somewhat decoupled from the inner regions of the rod. Consequently, for a nuclear rod, the behavior of the cladding and inner region of the rod can be widely different during rapid thermal transients s departure from nucleate boiling (DNB) or rod quench events.

It is the intent of this section to investigate the simulation capabilities of solid type heater rods to reproduce nuclear rod behavior. To accomplish this, it will be necessary to develop a method by which a powering scheme can be derived that will force the electric rod to duplicate pre-determined nuclear rod surface boundary behavior.

7.1 Zero Power Response

As discussed in Section 4 the general heat conduction differential equation can be written in the following form:

$$D(T) \equiv \nabla \cdot (k \nabla T) - \gamma \frac{\partial T}{\partial t} = -q''' \tag{23}$$

In cylindrical geometry with azimuthal symmetry and no axial heat conduction, the above equation simplifies to:
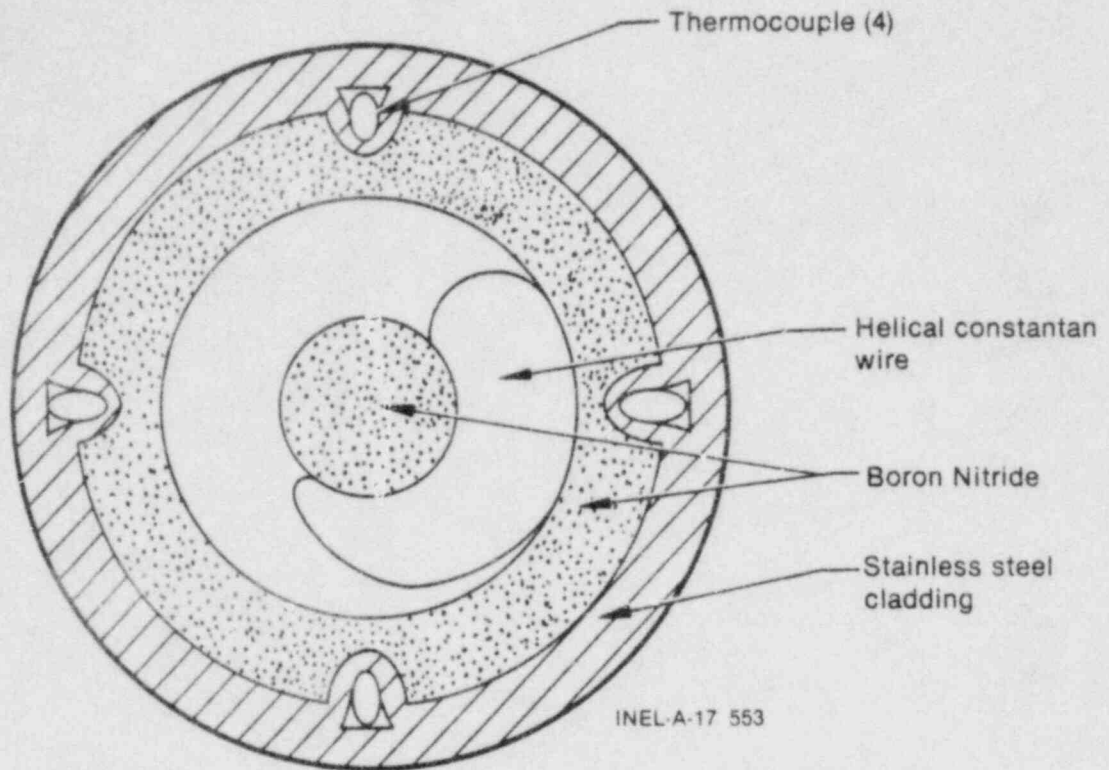
Fig. 4. A cross section of the Semiscale (solid type) heater rod.
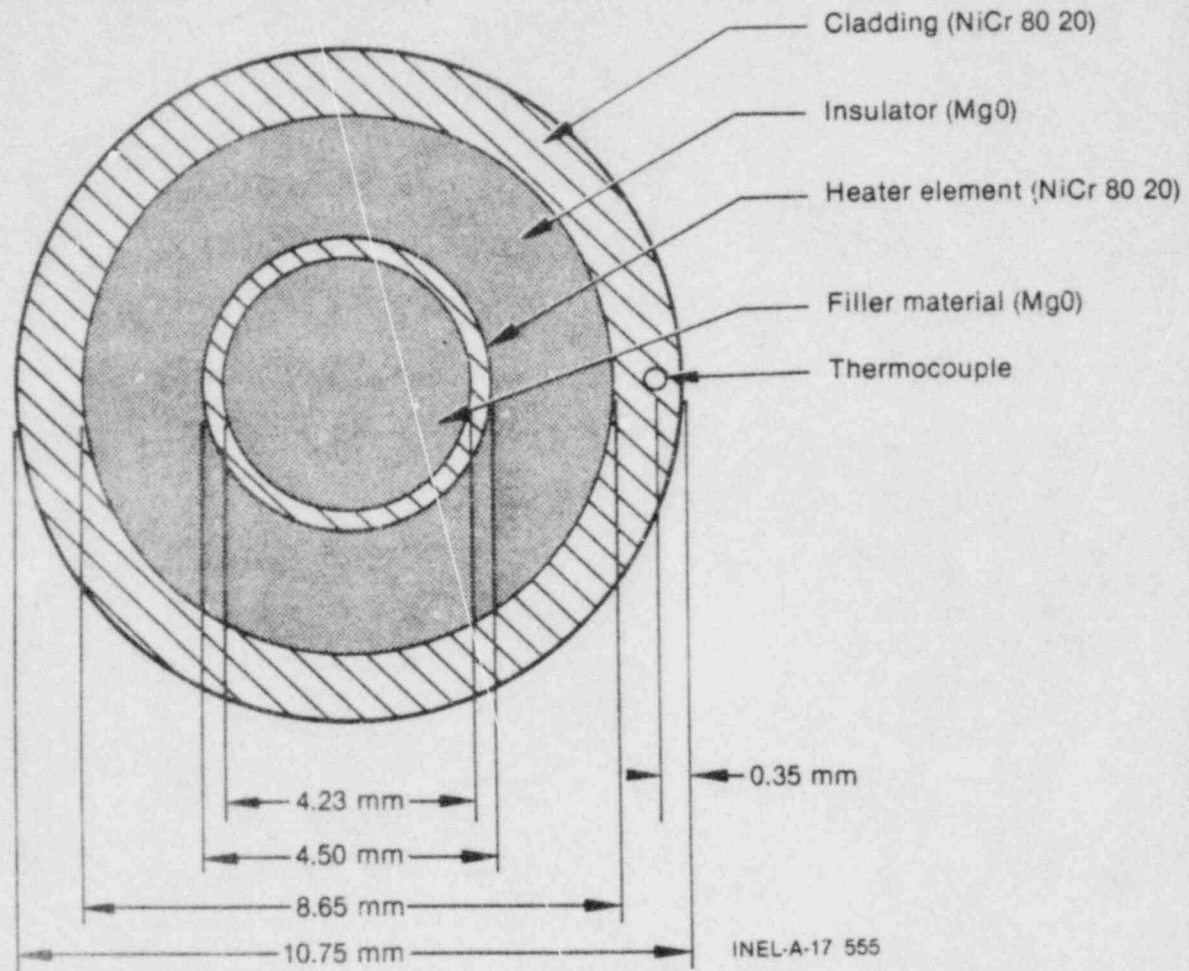
Fig. 5. A cross section of the FEBA (solid type) heater rod.
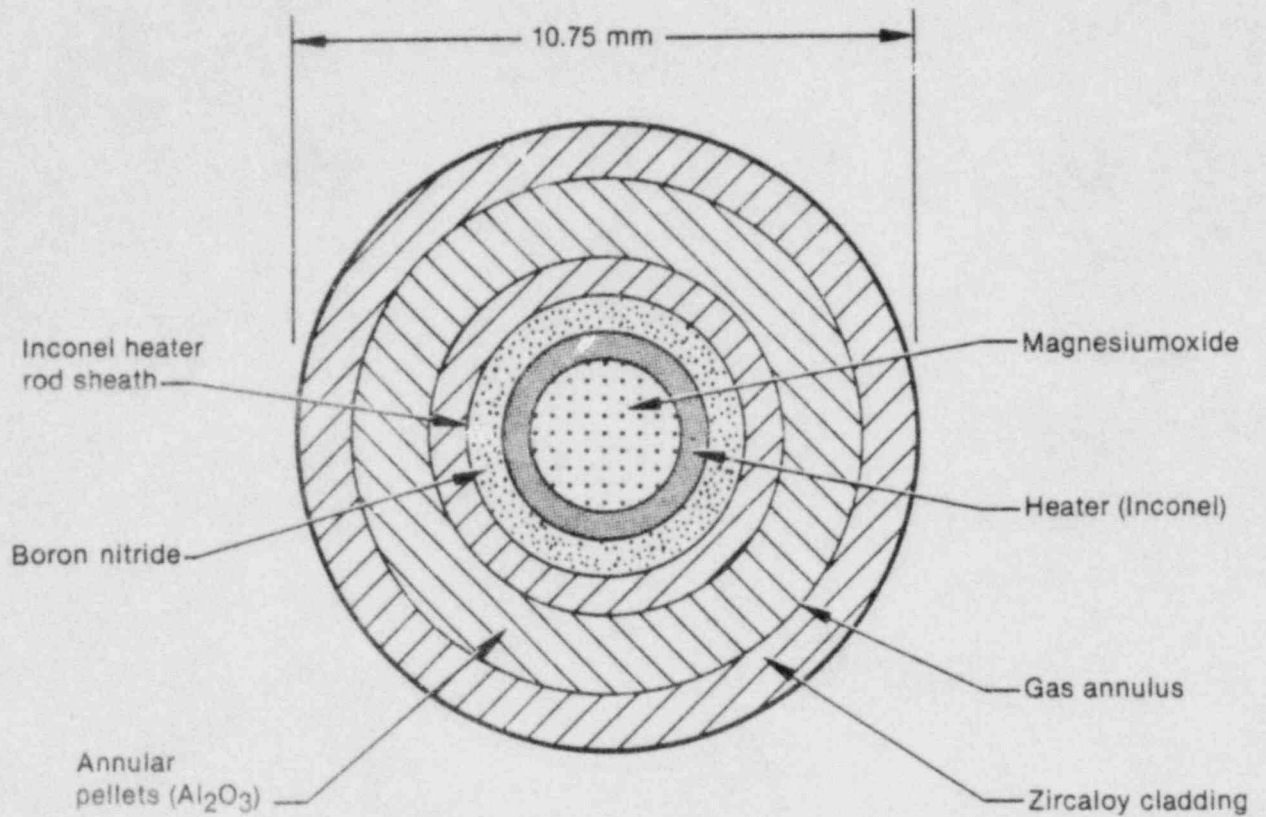
Fig. 6. A cross section of the Rebeka (cartridge type) heater rod.

$$D(T) \equiv \frac{1}{r} \frac{\partial}{\partial r} (r k\ \partial T/\partial r) - \gamma \frac{\partial T}{\partial t} = -q'''(r,t) \tag{24}$$

Again, the principal problem is to determine a function q_E''' for the electric rod such that the electric rod surface temperature and surface heat flux duplicates that of a nuclear rod. Before we attempt to solve this problem, it would be informative to first look at the temperature response of a heater rod subjected to the nuclear heat flux boundary condition and zero transient heater rod power. This is considered the "natural" or unforced response of the rod for a given surface boundary condition. It is the unforced response of the rod which plays an important part in determining the electric rod heat source term q_E''' in the general case.

Figures 7 and 8 illustrate the calculated inner surface cladding temperature and the associated heat flux delivered to the cladding of a nuclear rod du the LOFT L2-3 test. These figures represent target curves for the electric rod. The immediate objective of the exercise is to see how the "natural" or zero power response of an electric rod compares with the "natural" response of a nuclear rod, when the nuclear heat flux boundary condition is assumed for the electric rod at the inside cladding radius of the rod. For this introductory problem it is advantageous to select the electric rod heat flux boundary condition at the inside cladding radius instead at the rod surface. Notice, however, that if the electric rod has zircaloy cladding, and if we can match the nuclear rod heat flux and temperature conditions at the inside cladding radius, then the surface cladding boundary conditions must also match for both rods.

Before proceeding, it should be reiterated that the heat conduction differential equation is non-linear in the variable T whenever k and γ are functions of T. To avoid material temperature feedback effects it will be assumed here that k and γ are constants. In this way we can study how overall changes in rod thermal conductivity, with a fixed γ, affect the
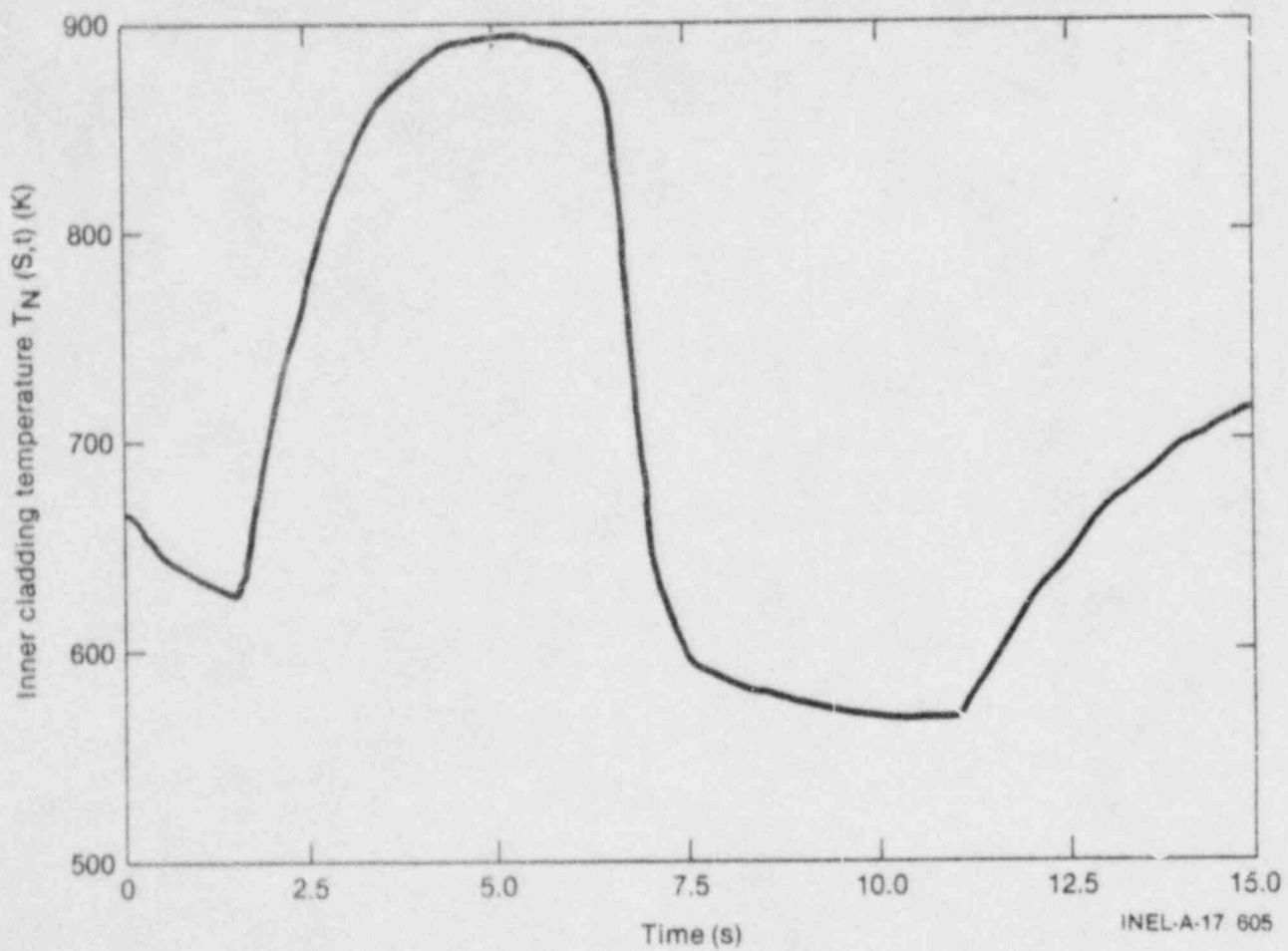
Fig. 7. A FRAP-T5 calculated inner cladding temperature $(T_N(S,t))$ for the hot axial node of a high powered nuclear rod (39.4 kW/m) during the LOFT L2-3 experiment. For this case, the inside radius (I.R.) of the cladding is $S = 0.475$ cm.
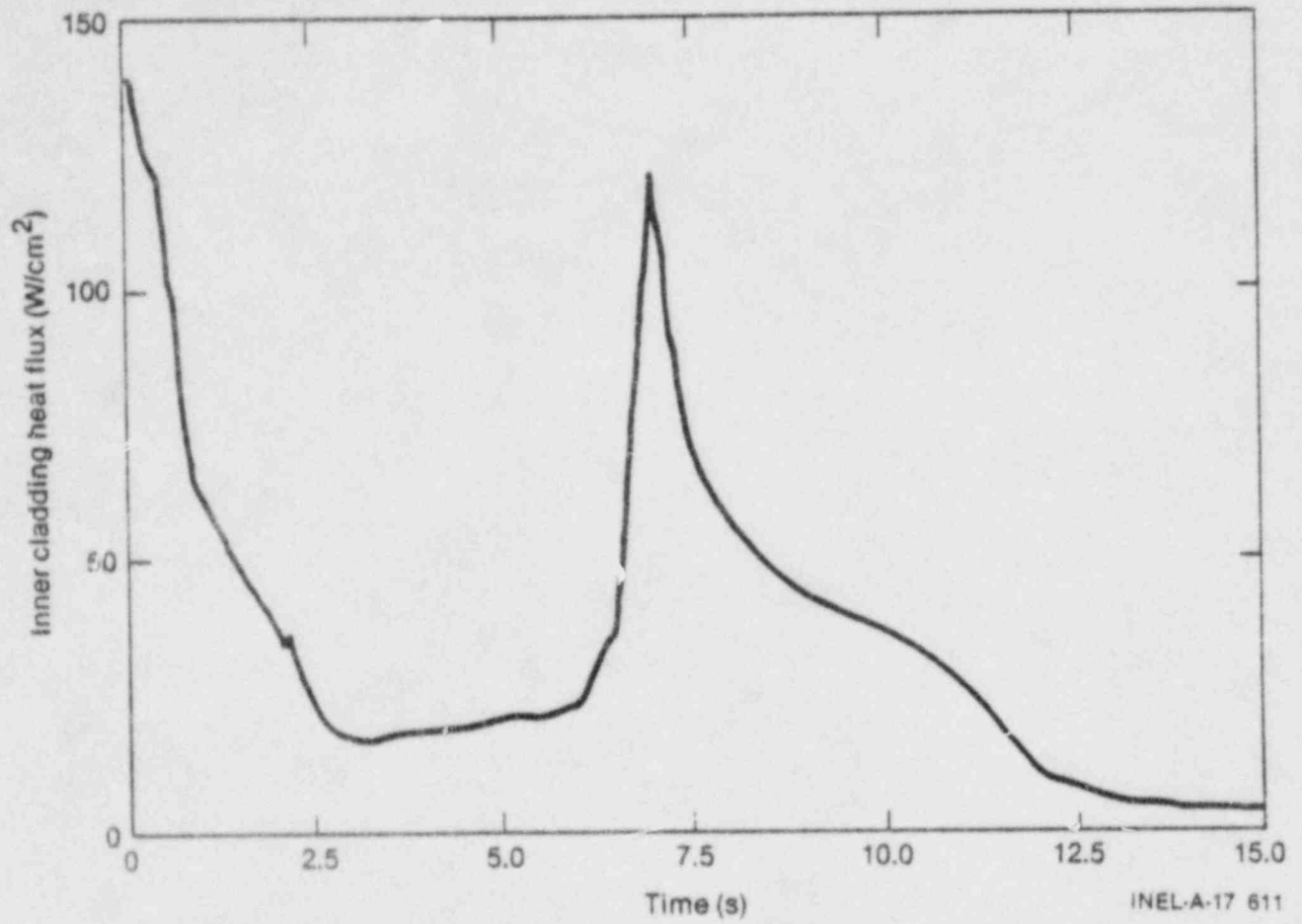
Fig. 8. The calculated heat flux $(\phi_N(S,t))$ delivered to the cladding of the LOFT nuclear rod described in Fig. 7.

temperature response of an electric rod undergoing nuclear heat flux cooling and zero transient rod power. Figure 9 shows a typical homogeneous electric rod design that was considered for this calculation.
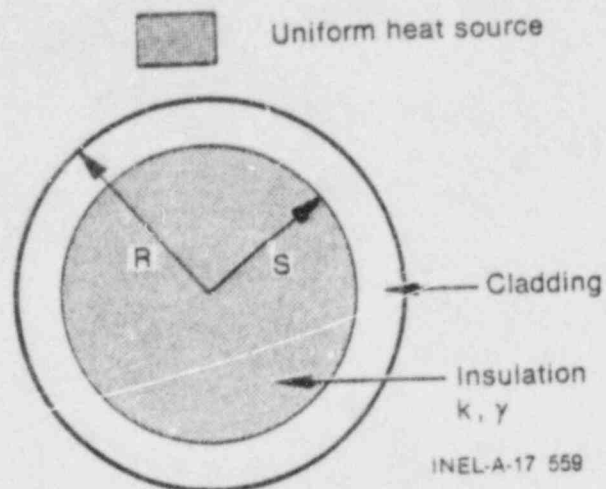
Fig. 9. An electric rod model of a solid type heater rod with no transient heat source and constant material properties. During steady state the insulation pellet is assumed to be uniformly heated. S equals the inside cladding radius of the rod where the nuclear heat flux boundary condition is assumed, e.g. $\phi_E(S,t) = \phi_N(S,t)$.

Using the HEATO conduction code,[6] a series of calculations were made for the above electric rod assuming various insulator thermal conductivities, and a fixed volumetric specific heat ($\gamma = 3.7$ J/cm^3-K). Further, each calculation was made assuming the existence of a steady state condition prior to t = 0, and an inside cladding heat flux equal to that presented in Figure 8 for the LOFT L2-3 nuclear rod. The results of the calculations are shown in Figure 10. Aside from an arbitrary vertical off-set, which is made to simply separate the individual curves, Figure 10 shows the relative cooling behavior of a solid type heater rod for various thermal conductivities under zero transient power.
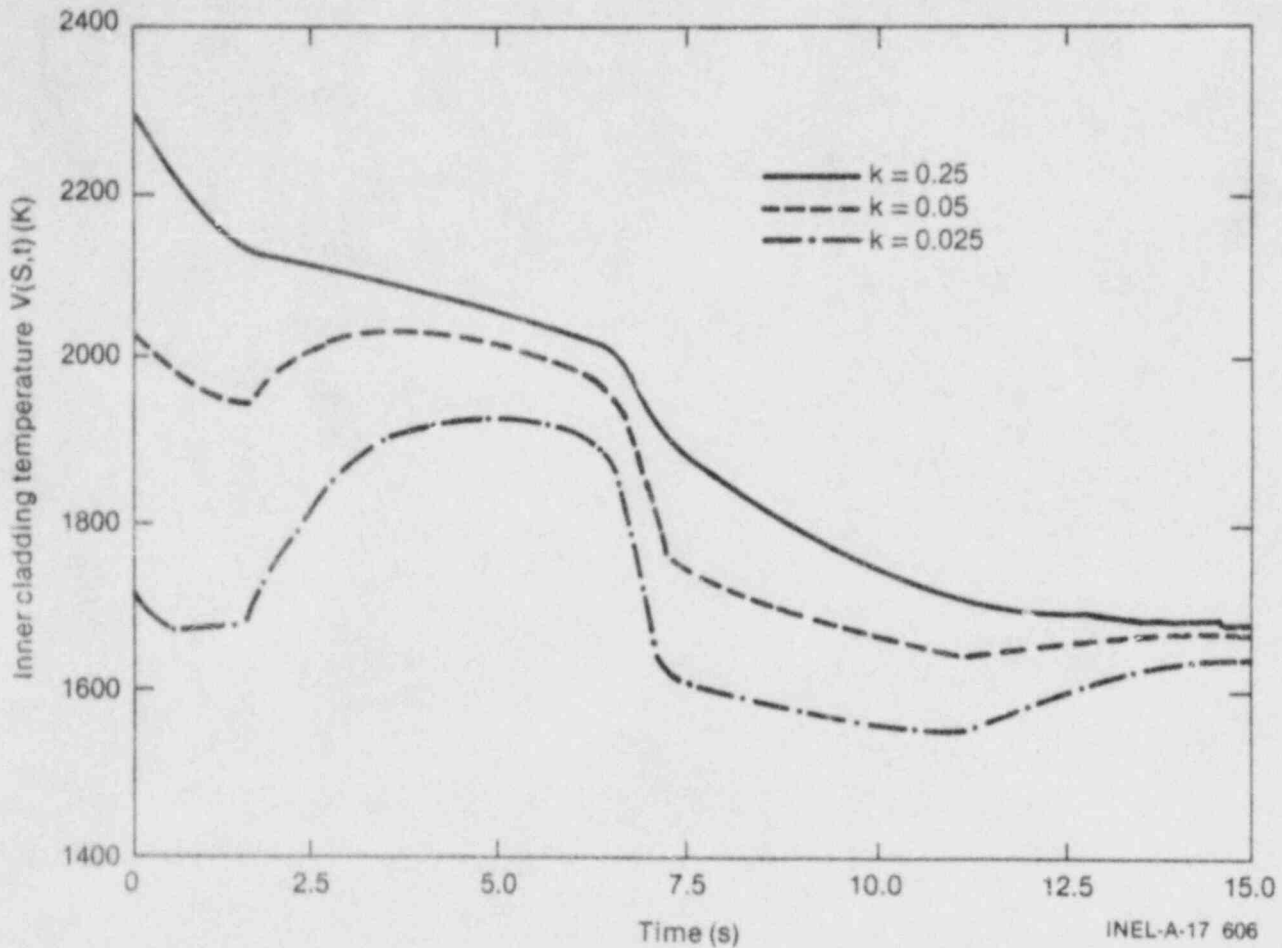
Fig. 10. An illustration of the relative cooling behavior of various types of solid type heater rods of different insulator thermal conductivities, and the same volumetric specific heat $\gamma = 3.7$ J/cm^3-K . Calculations are based on the nuclear heat flux boundary condition shown in Fig. 8. The shape of the lowest curve (k = 0.025 W/cm-K) approximates that of a nuclear rod.

31

Since k and γ are assumed to be constants, therefore, independent of temperature (T), the heat conduction operator D will also be independent of the variable T. Therefore, no material temperature feedback exists. Consequently, it is the general shape of the curves presented in Figure 10 that is important, not the absolute numerical values.

From Figure 10 it is evident that as k is decreased from 0.25 W/cm-K to 0.025 W/cm-K, the temperature response curve more closely approximates the general shape of the LOFT nuclear rod temperature response. Furthermore, on close examination of Figure 10, it is clear that the maximum cooldown behavior of the solid type heater rods of high internal thermal conductivity are not as large as that of the lowest curve (k = 0.025), which most closely represents the nuclear rod case. Since only positive internal rod power can be realistically produced inside an electric rod, it is apparent that the heatup rates evident in the curves of Figure 10 can be easily increased by adding power to the rod; however, doing this can only aggreviate or decrease the electric rod cooldown rate later cn. Therefore, it appears that the electric rods can be forced to heatup at nearly any prescribed rate; however, the cooldown rate is limited by the rod design and the previous power history of the rod.

The preliminary data discussed here tends to indicate that the cladding of a homogeneous solid type heater rod of high internal thermal conductivity cannot cool down as quickly as a nuclear rod. This basic conclusion will be supported by more detailed data that is presented later on.

Two general facts that can be summarized from the above discussion and Figure 10 are:

1. Under zero transient rod power, the maximum cooldown rate is achieved for the rod; and that this rate is influenced by the rod thermal conductivity (k). The general rule is that as k

32

increases, the maximum surface cladding cooldown rate decreases. These conclusions are based on a fixed surface heat flux boundary condition. That is, by allowing the rod surface heat flux to change, one can also influence the rod cooldown rate.

2. Adding power to an electric rod can help increase cladding heatup rates, however, doing this will only decrease the optimal cooldown rate later on.

7.2 Homogeneous Heater Rod Theory

We presently investigate how it is possible to calculate an electric rod power for a homogeneous rod that will allow the rod to simulate the surface behavior of a nuclear rod when the surface thermal-hydraulic boundary conditions for both rods are the same. In order to do this we need to use the "zero power response" concept introduced in the previous section. To begin, let

S = the inside radius of the nuclear or electric rod cladding

$\phi_N(S,t)$ = the nuclear rod boundary heat flux (as a function of time) at $r = S$

$\phi_E(S,t)$ = the electric rod boundary heat flux at $r = S$

$T_N(S,t)$ = the nuclear rod inside cladding temperature

$T_E(S,t)$ = the electric rod inside cladding temperature.

Figure 7 illustrates a typical LOFT L2-3 (hot pin) inner cladding temperature, and Figure 8 the corresponding nuclear heat flux. These figures represent target curves for the electric rod. A method will be described showing how a power function can be calculated for the Semiscale heater rod so that the Semiscale rod can match the boundary conditions of

33

the nuclear rod. Since the Semiscale heater rod involves several different regions of various dimensions, material properties, and a heater element that is embedded inside the rod, it is not possible to immediately solve the problem for this complicated rod design. Instead, a more simple rod design is first studied, and then the solution for this geometry is applied to the more complex rod.

Figure 11 shows a simple "homogenized" model of the Semiscale rod. In the "homogenized" model, the heated region is uniformly distributed across the rod insulation ($r < S$) and averaged values for k_E and γ_E are assumed for the entire insulation of the electric rod. We now proceed to solve for the appropriate rod power function of the simple homogeneous rod model when the appropriate boundary conditions are specified at $r = S$; and then apply the technique to the more complicated rod design.
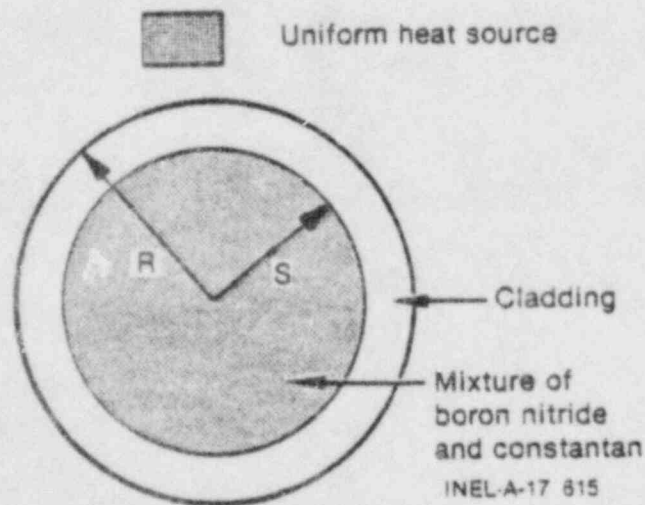
Fig. 11. A homogenized model of the Semiscale heater rod where the boundary conditions (Figures 7 and 8) are specified at the insulator surface $r = S$.

34

First, define:

$$T(r,t) = T_N(S,t) + V(r,t) - V(S,t) \qquad (25)$$

where $V(r,t)$ is that electric rod temperature function which satisfies the following problem:

$$D_E(V) = \begin{cases} \dfrac{-2\ \phi_N(S,0)}{S} & t \le 0 \quad \text{(steady state)} \qquad (26a) \\[2ex] 0 & t > 0 \quad \text{(transient)} \qquad (26b) \end{cases}$$

subject to the boundary condition:

$$-k_E \left.\frac{\partial V}{\partial r}\right|_{S,t} = \phi_N(S,t). \qquad (26c)$$

Here, $V(r,0)$ is uniquely determined by the steady state solution to Equation (26a) when $V(S,0)$ is specified. Notice that Equation (25) is very similar to Equation (14) for the Zaloudek heater rod.

The $V(r,t)$ function describes the "natural" electric rod temperature response, without material temperature feedback, subject to a nuclear heat flux boundary condition and zero transient power. Determination of V is very similar to the exercise performed in Section 7.1.

Using the HEATO code it is quite easy to solve problem (26) and determine the function $V(r,t)$. It should be pointed out, however, that due to a peculiarity in the HEATO code, negative temperatures are not possible. Therefore it might be necessary to initialize the HEATO calculation from an arbitrarily high initial temperature distribution by selecting a high value for $V(S,0)$. In this way, negative or near zero rod temperatures [$V(r,t)$]] can be avoided. Since k_E and γ_E are constants,

no material temperature feedback exists in the solution temperature $V(r,t)$. Therefore, the shape of the solution function is independent of the initial temperature selection of $V(S,0)$. Furthermore, since it is the shape of the solution which is important and not the actual numerical values of the solution, the above method adequately determines an appropriate V temperature function. That is, the function $V(r,t)$ is determined to within an arbitrary constant $V(S,0)$.

Now, using Equation (25) notice that:

$$T(S,t) = T_N(S,t) \tag{27a}$$

and $\frac{\partial T}{\partial r} = \frac{\partial V}{\partial r}$, which implies that

$$\phi(S,t) = -k_E \left. \frac{\partial T}{\partial r} \right|_{S,t} = -k_E \left. \frac{\partial V}{\partial r} \right|_{S,t} = \phi_N(S,t) \tag{27b}$$

Therefore, Equations (25) and (26) specify a function $T(r,t)$ that has the same boundary temperature and boundary heat flux as the nuclear rod. Now, operating on both sides of Equation (25) with the D_E operator, and using the fact that D_E is linear, we find that during the transient $(t > 0)$:

$$D_E(T) = D_E[T_N(S,t)] + D_E[V(r,t)] - D_E[V(S,t)]$$

$$= -\gamma_E \frac{\partial T_N(S,t)}{\partial t} + 0 + \gamma_E \frac{\partial V(S,t)}{\partial t}$$

$$= -\gamma_E \frac{\partial}{\partial t} [T_N(S,t) - V(S,t)] \tag{28}$$

Since $D_E(T) = - q_E'''$, then the transient power is:

$$q_E'''(t) = \gamma_E \frac{\partial}{\partial t} [T_N(S,t) - V(S,t)] \quad \text{(for } t > 0 \text{ and boundary conditions specified at } r = S). \tag{29}$$

Equation (29) describes the transient uniform power density for the homogeneous rod model when the rod boundary conditions are specified at $r = S$. The steady state power density (for $t \leq 0$) is also easily calculated and is:

$$q_E'''(0) = \frac{2 \phi_N(S,0)}{S} \tag{30}$$

The two results, (29) and (30), define the entire time dependent rod power density function (for the particular axial node under consideration):

$$q_E'''(t) = \begin{cases} \dfrac{2 \phi_N(S,0)}{S} & t \leq 0 \text{ (steady state)} \tag{31a} \\[2em] \gamma_E \dfrac{\partial}{\partial t} [T_N(S,t) - V(S,t)] & t > 0 \text{ (transient)} \tag{31b} \end{cases}$$

When the rod boundary conditions are specified at $r = R$ instead of $r = S$, then the appropriate power function can be determined by substituting R for S in Equations (31a) and (31b).

It is possible to incorporate the steady state power solution as just a special case of the transient, and thereby allow for a more general formula where (31b) actually represents the transient and steady state powers, however, to do this one must allow for the uncomfortable result that the time derivative of the function $[T_N(S,t) - V(S,t)]$ is non-zero during the steady state period. This result can occur if V(S,t) is allowed

to be non-constant during steady state.* Because one would normally like all time derivatives of functions to be zero during steady state conditions, we have elected to represent $q_E'''(t)$ in terms of two parts, a true steady state term and a transient term, thereby avoiding this problem.

It should also be pointed out that it is not really necessary to assume that k_E and γ_E are constants in order to solve the above problem. All that is really necessary is that k_E and γ_E are independent temperature. For instance, had we assumed that k_E and γ_E were functions of r and t, e.g., $k_E = k_E(r,t)$ and $\gamma_E = \gamma_E(r,t)$, then the transient rod power density would have been:

$$q_E'''(r,t) = \gamma_E(r,t) \frac{\partial}{\partial t} [T_N(S,t) - V(S,t)] \tag{32}$$

Unless $\gamma_E(r,t)$ is a separable function of its space and time variables, q_E''' will generally depend upon both r and t and will not be a separate function. If γ_E can be treated as only a function of r, then

$$q_E'''(r,t) = \gamma_E(r) \frac{\partial}{\partial t} [T_N(S,t) - V(S,t)] \tag{33}$$

According to Equation (33), $q_E'''(r,t)$ can be written as the product of two factors: $P(r)$ and $Q(t)$ where

$$P(r) = \gamma_E(r) \tag{34a}$$

$$Q(t) = \frac{\partial}{\partial t} [T_N(S,t) - V(S,t)] \tag{34b}$$

---

* This is done by selecting zero as the steady state power in (26a) instead of $2 \phi_N(S,0)/S$.

38

Here, P(r) represents the radial power profile function and Q(t) the time dependent power factor. Since all realistic electric rod designs position heater elements at discrete locations inside the rod, only certain separable power functions are possible. In other words, arbitrary power functions $q_E'''(r,t)$ are not permissible since heat can be generated at only the heater rod element locations. Hence, if $q_E'''(r,t) = P(r) Q(t)$, then P(r) is fixed by the design of the rod and Q(t) is the only free unassigned function we can define.

For the remaining analysis we shall restrict our solutions to only separable power functions. Please note that the uniform power solution obtained in Equation (31) is a separable function since γ_E is a constant, and the heater element region is assumed to be uniformly distributed across the rod.

There is another important item that should be pointed out at this time. Namely, what would have happened had we selected a non-zero but uniform time dependent power function instead of the zero transient power that was selected in Equation (26b)? How would this have affected the calculation of $T(r,t)$ and $D_E(T)$? Since it can be shown that the functions T and $q_E''' = -D_E(T)$ are uniquely determined by the boundary and initial conditions, then changing $D_E(V)$ will not affect the calculation or $D_E(T)$. That is, $q_E'''(t)$ and $T(r,t)$ are invariant to changes made in the uniform transient power selection that defines V. Therefore, we could have selected some other function for $D_E(V)$ and expected to obtain the same result for T and $D_E(T)$. The reason that $D_E(V) = 0$ was selected as the transient power is due to its simplicity; however, it sometimes occurs that another more convenient transient power selection should be made. For instance, for calculational purposes it might be best to select:

$$D_E(V) = \gamma_E \frac{\partial T_N(S,t)}{\partial t} \qquad (t > 0) \qquad (35)$$

39

So that,

$$D_E(T) = - \gamma_E \frac{\partial T_N(S,t)}{\partial t} + \gamma_E \frac{\partial T_N(S,t)}{\partial t} - \gamma_E \frac{\partial V(S,t)}{\partial t}$$

$$= - \gamma_E \frac{\partial V(S,t)}{\partial t} \tag{36}$$

The function $V(r,t)$ derived from the differential Equation (35), subject to the steady state power condition (26a) and the nuclear heat flux condition (26c) will differ from the original $V(r,t)$ function determined from system (26), however, evaluation of $q_E = -D_E(T)$ and T [from Equation (36)] will result in the same functions as before.

To demonstrate how the method des ribed by Equations (26) and (29) are applied, a simple example is considered. Recall Figure 10. This figure illustrated the zero power or "natural" response of a homogeneous electri, rod for various thermal conductivities, assuming a nuclear heat flux boundary condition at $r = S$. This is exactly what is called for in solving system (26) to determine $V(S,t)$. Next, according to formula (29) the required uniform power density necessary to duplicate the additional ·_iperature boundary condition $T_N(S,t)$, is easily computed to be:

$$q_E'''(t) = \gamma_E \frac{\partial [T_N(S,t) - V(S,t)]}{\partial t} \tag{37}$$

where

γ_E = 3.7 J/cm^3-k (for these cases)

$T_N(S,t)$ is given in Figure 7

$V(S,t)$ is given in Figure 1G

40

Doing the appropriate calculations, the required difference functions $[T_N(S,t) - V(S,t)]$ are displayed in Figure 12.

Inspection of the response functions displayed in Figures 12, and formula (37) for the desired power density function shows that unrealistic negative rod powers occur whenever the derivative of the response temperature $[T_N(R,t) - V(R,t)]$ is negative. Inspection of Figure 12 shows that negative temperature slopes are prominent during part of the transient for two of the three cases. The negative rod powers occur becau᠁ᦙ of the relatively high rod thermal conductivities, which allows thᦙ ᦙ stored energy to be quickly transported to the rod surface. Only in one case does the rod input power function remain essentially non-negative throughout the transient, and this occurs for a case for which the rod thermal conductivity ($k_E = 0.025$ W/cm-k) is similar to that of UO_2.

It is quite clear from the observations made above that a homogeneous electric rod with a uniform power source might require negative rod powers to properly match rapid ᥎uclear rod cooling boundary conditions when the electric rod material thermal conductivity differs greatly from that of a nuclear rod. This very same observation will be pointed out again as the behavior of more complicated electric rod models are studied.

7.3 Heterogeneous Heater Rod Theory

The purpose of this section is to develop a technique for extending the results of the previous section to cover a more complicated electric rod design, e.g., the Semiscale heater rod. Figures 13 and 14 compare a homogeneous or uniformly distributed heat source (UDHS) model and a heterogeneous or standard model of the Semiscale heater rod.
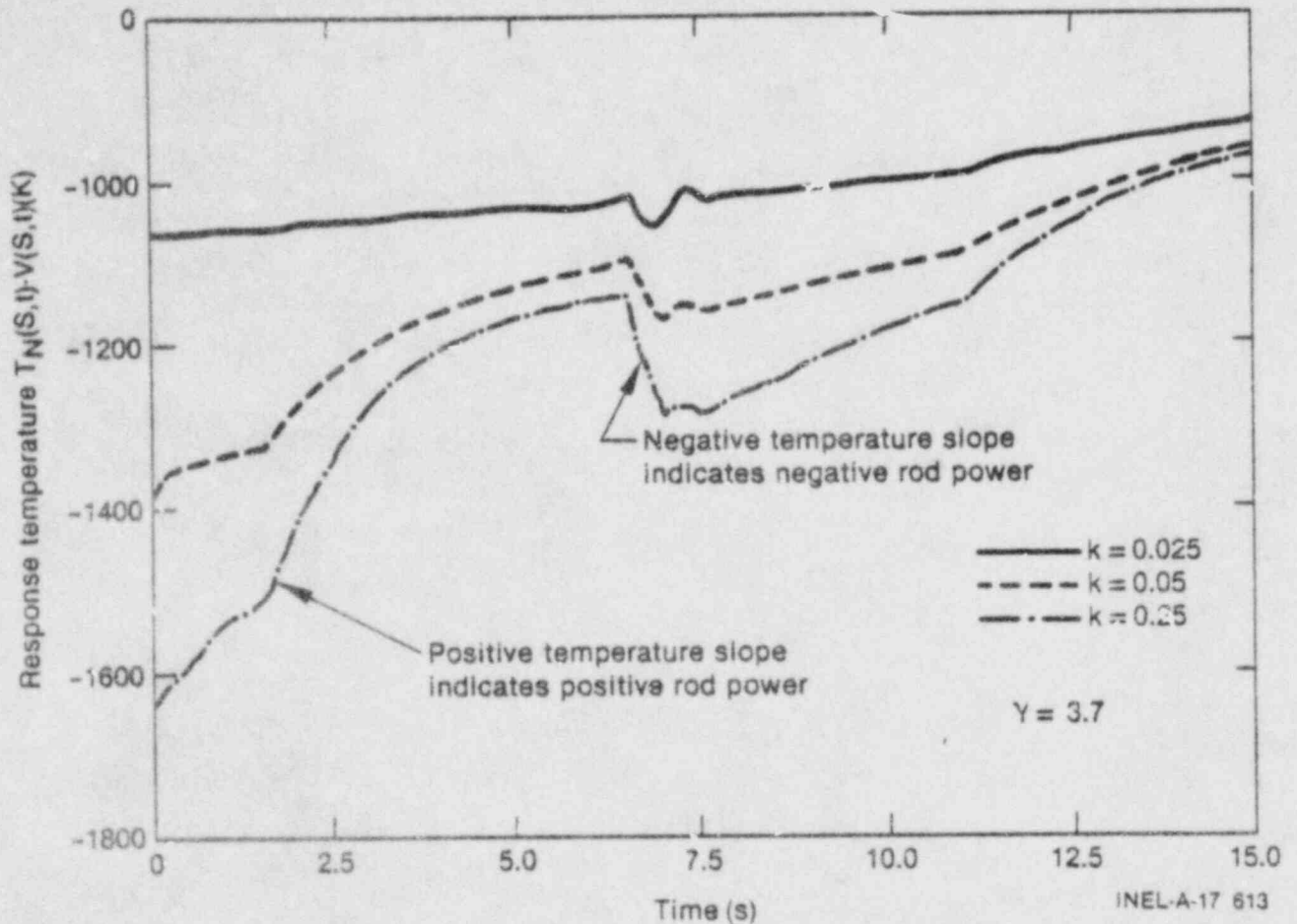
Fig. 12. The response temperature $(T_N(S,t) - V(S,t))$ for the heater rod designs considered in Fig. 10. Any decrease in the response temperature indicates that a negative electric rod input power is required to match the specified nuclear rod boundary conditions. Since the average thermal conductivity of the Semiscale rod insulation is between 0.05 and 0.25, it appears that the input power to the Semiscale rod needed to duplicate the LOFT nuclear rod boundary conditions should also be negative between 6.5 and 7.0 seconds.
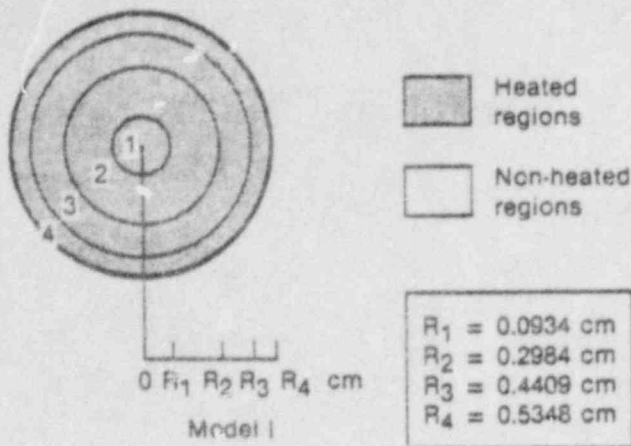
Fig. 13. A uniformly distributed heat source model of the Semiscale heater rod. The material properties of regions 1 thru 4 are assumed to be temperature independent.
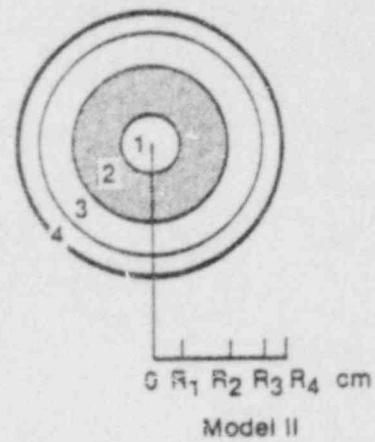
Fig. 14. A heterogeneous or discrete heater element model of the Semiscale heater rod. The material of regions 1 thru 4 are assumed to have standard Semiscale temperature dependent properties.

$R_1 = 0.0934$ cm	
$R_2 = 0.2984$ cm	
$R_3 = 0.4409$ cm	
$R_4 = 0.5348$ cm	

INEL-A-17 556

Using the technique developed for a homogeneous rod with a uniform power distribution, it is quite simple to calculate a rod power density function $P_I(t)$ for the Model I rod that forces the rod to match two prescribed surface boundary conditions. In order to solve the same problem for the heterogeneous (Model II) rod we make the initial estimate that the heterogeneous heater element power density function $P_{II}(t)$ is proportional to $P_I(t)$, where the proportionality constant is A/A_h. Here, A represents the cross sectional area of the rod ($A = \pi R_4^2$), and A_h represents the cross sectional area of the heater element region [$A_h = \pi (R_2^2 - R_1^2)$]. For the Semiscale rod $A/A_h = 3.56$. Therefore,

$$P_{II}(t) = 3.56\, P_I(t) = 3.56\, \gamma_E \left. \frac{\partial[T_N(R,t) - V(R,t)]}{\partial t}\right|(R = R_4) \tag{38}$$

43

Here $V(R,t)$ is determined by solving the homogeneous heater rod problem, e.g. system (26) for Figure 13.

Equation (38) is based on a conservation of energy model; that is, the total linear energy delivered to the heterogeneous rod model $[P_{II} \cdot \pi (R_2^2 - R_1^2)]$ should be approximately equal to the total linear energy delivered to the UDHS model $(P_I \cdot \pi R_4^2)$. However, since energy deposited in the heater element of the Model II rod does not instantaneously affect the surface boundary conditions of the rod, Equation (38) should be modified to take into account this time delay. Let τ represent the effective response time of the Semiscale rod, then a better estimate for P_{II} is:

$$P_{II}(t) = 3.56 \, P_I(t + \tau) \tag{39}$$

Although τ is itself temperature dependent, to a good approximation it can be assumed to be constant. Without going into details, estimates have already been made for the effective response time of the Semiscale heater rod and these calculations indicate that τ is approximately 0.2 seconds. Consequently, it takes about 0.2 seconds for a change in heater rod power to manifest itself as a significant change in the rod surface temperature or heat flux. Therefore, for the Semiscale rod:

$$P_{II}(t) = 3.56 \, P_I \, (t + 0.02) \tag{40}$$

Equation (40) should in theory be a reasonably accurate estimate of the correct rod power function, however, because the UDHS model is not a highly accurate description of the Semiscale rod, the power function $P_{II}(t)$ might need modification. Generally, $P_{II}(t)$ is treated as the

44

second estimate $[Q_2 = P_{II}(t)]$ of the correct rod power function.* Subsequent rod power estimates are based on the previous power estimates using the algorithm developed below.

Modification of $Q_2 = P_{II}(t)$ is made as follows. Using a standard HEATO (Model II) description of the Semiscale rod (see Appendix B) calculate the surface rod temperature based on (a) the heater rod power density $Q_2(t)$, and (b) the orginal surface heat flux boundary condition. The resulting temperature (T_{E2}) is then used to correct the power density function as follows: First compute the difference (V) between the desired $[T_N(R,t)]$ and the calculated surface cladding temperatures $[T_{E2}(R,t)]$.

$$V(R,t) = T_N(R,t) - T_{E2}(R,t)$$

Then use the $V(R,t)$ function to estimate the change in rod power needed to produce this observed difference. An estimate of this power is:

$$\Delta P_2(t) = \gamma_E \; (\frac{A}{A_h}) \; \frac{\partial \; V(R,t)}{\partial t} = C \; \frac{d \; V(R,t)}{dt} \tag{41}$$

For the Semiscale rod $C = \gamma_E \cdot (A/A_h) = (3.7)(0.897/0.252) =$ 13.17. Next, shift the $\Delta P_2(t)$ power function by $\tau = 0.2$ seconds to compensate for the finite rod response time, and then add this result to the initial power estimate Q_2 to obtain:

$$Q_3(t) = Q_2(t) + \Delta P_2(t + \tau) \tag{42}$$
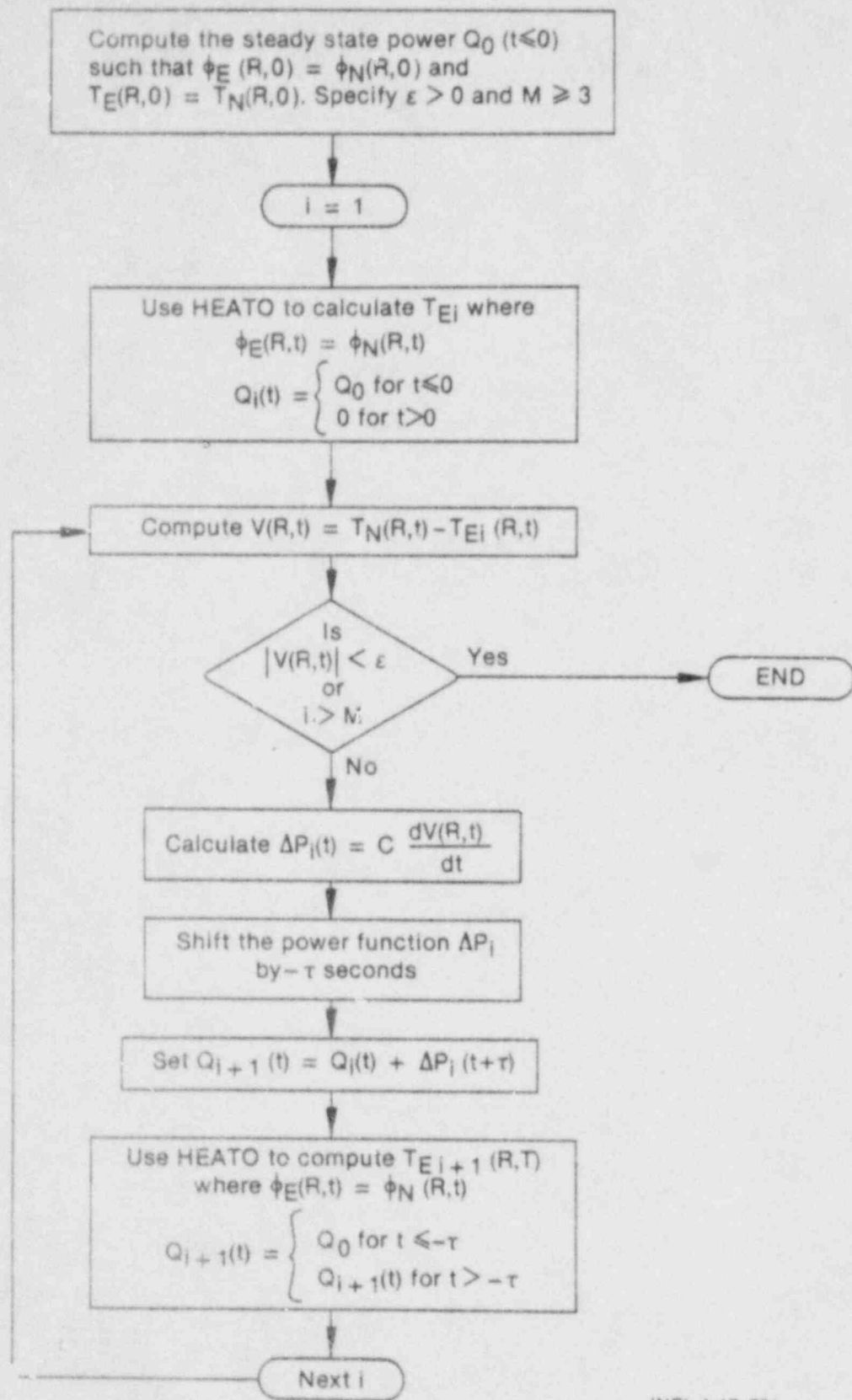
---

* The first estimate is $Q_1(t) = 0$ for $t > 0$.

Now, the heater rod power density function $Q_3(t)$ should represent a better estimate of the desired rod power function than $Q_2(t)$, but this also might not be good enough. Therefore, repeat the process starting with $Q_3(t)$ as the original power estimate and recompute a new temperature difference $T_N(R,t) - T_{E3}(R,t)$ and a corresponding power $\Delta P_3(t+\tau)$ and finally a new power density function $Q_4(t)$. Repeat the process as many times as is necessary until the difference between the desired and calculated surface cladding temperatures is as small as desired, or after a reasonable number of iterations have been made.

Experience has shown that the above process should converge rapidly and that a good power estimate can be made by the third or fourth iteration. Figure 15 presents a flowchart illustrating the entire algorithm.

7.3.1 Determination of the Local Semiscale Rod Power Needed to Reproduce the LOFT L2-3 Nuclear Rod Response

Figures 16 and 17 show the measured surface cladding temperature and the calculated surface cladding he. flux of a nuclear rod during the LOFT L2-3 test. These figures represent "target" curves for the Semiscale heater rod and the problem at hand is to determine a local rod power for the Semiscale heater rod that will reproduce this surface rod behavior.

Using the technique explained above, a calculation is made for the zero power response of the Semiscale (Model I) rod using the nuclear heat flux as the surface boundary condition at $r = R = R_4$. The calculated surface cladding response is shown in Figure 18a where it is overlayed with the nuclear surface cladding temperature. The corresponding electric rod power function is shown in Figure 18b. Notice that the "natural" response of the Semiscale rod is greatly different than the nuclear rod. Consequently, it is necessary to find a power function for the Semiscale rod that will force the rod to duplicate the nuclear rod response.

46

Compute the steady state power Q_0 $(t \leqslant 0)$
such that $\phi_E(R,0) = \phi_N(R,0)$ and
$T_E(R,0) = T_N(R,0)$. Specify $\varepsilon > 0$ and $M \geqslant 3$

$i = 1$

Use HEATO to calculate T_{Ei} where
$\phi_E(R,t) = \phi_N(R,t)$

$Q_i(t) = \begin{cases} Q_0 \text{ for } t \leqslant 0 \\ 0 \text{ for } t > 0 \end{cases}$

Compute $V(R,t) = T_N(R,t) - T_{Ei}(R,t)$

Is
$|V(R,t)| < \varepsilon$
or
$i > M$

Yes → END

No

Calculate $\Delta P_i(t) = C \dfrac{dV(R,t)}{dt}$

Shift the power function ΔP_i
by $-\tau$ seconds

Set $Q_{i+1}(t) = Q_i(t) + \Delta P_i(t+\tau)$

Use HEATO to compute $T_{Ei+1}(R,T)$
where $\phi_E(R,t) = \phi_N(R,t)$

$Q_{i+1}(t) = \begin{cases} Q_0 \text{ for } t \leqslant -\tau \\ Q_{i+1}(t) \text{ for } t > -\tau \end{cases}$

Next i

INEL-A-17 751

Fig. 15. An algorithm for estimating the electric rod power needed to
duplicate two prescribed surface boundary conditions. For the
Semiscale heater rod $C = 13.17$ J/cm^3-K and $\tau = 0.2$ seconds.
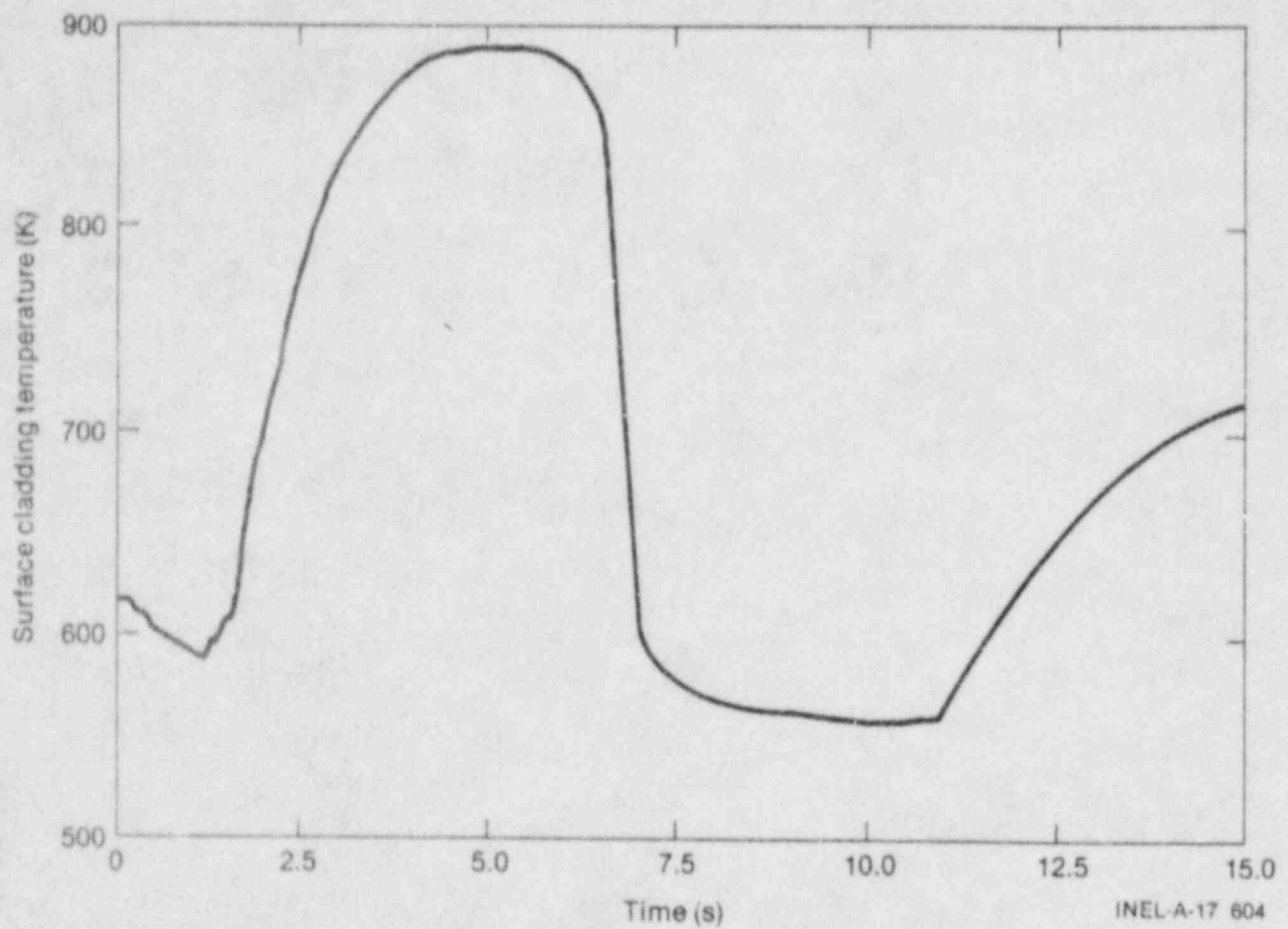
Fig. 16. A typical surface cladding measured temperature $(T_N(R,t))$ on a nuclear rod during the LOFT L2-3 experiment.
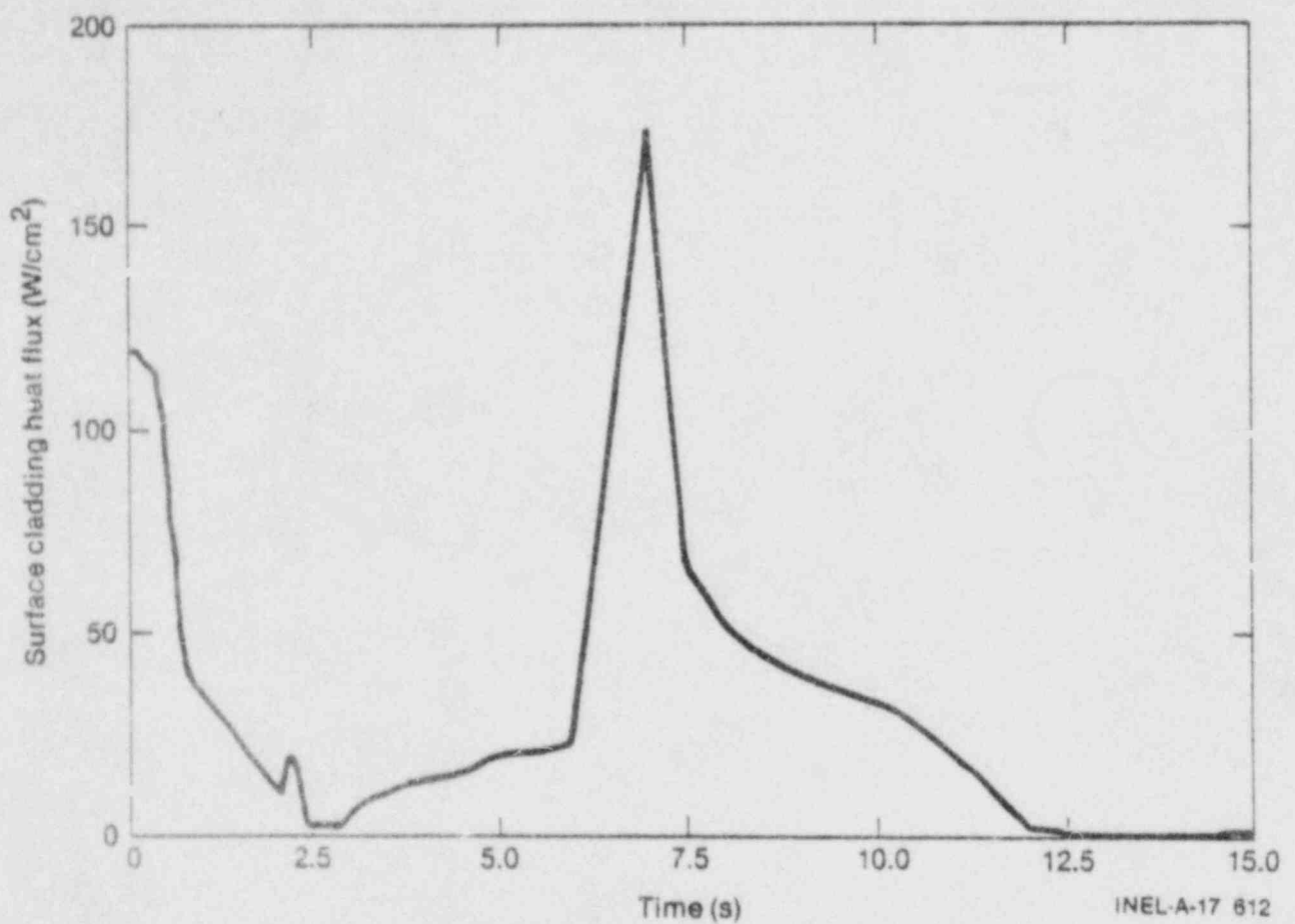
Fig. 17. The FRAP-T5 calculated surface cladding heat flux $(\phi_N(R,t))$ corresponding to the data shown in Fig. 16.

49

LO-14-81-074
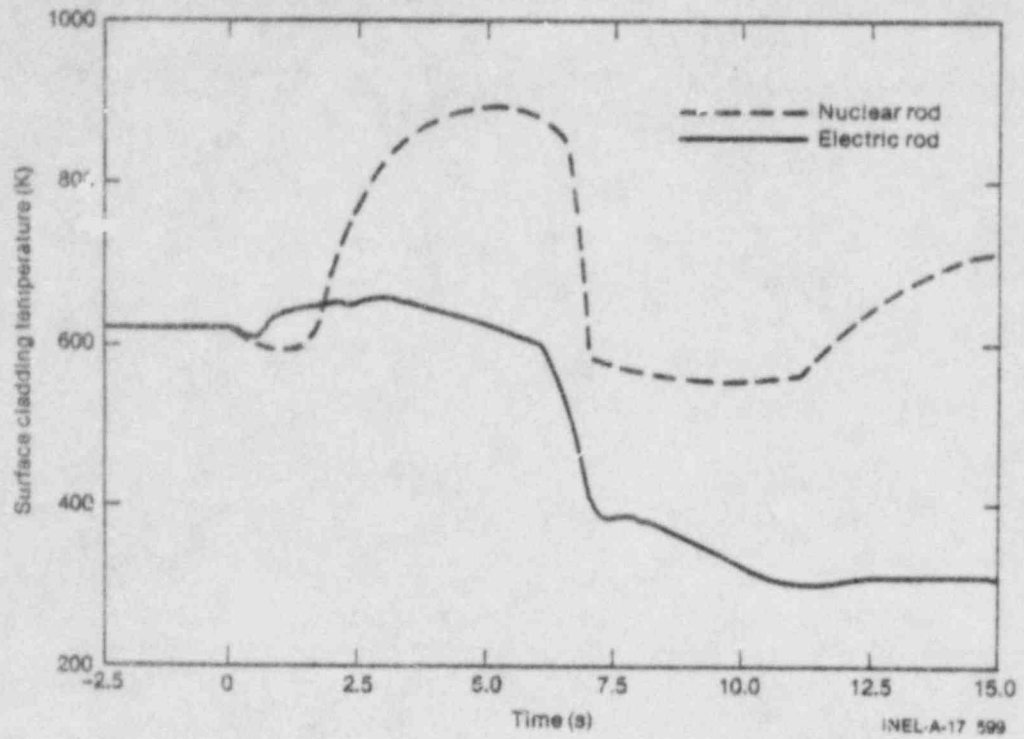
Fig. 18a. An overlay of the LOFT nuclear rod surface cladding temperature
and the corresponding Semiscale temperature response for a
zero rod transient power condition, shown in Fig. 18b.
(Calculation 1)
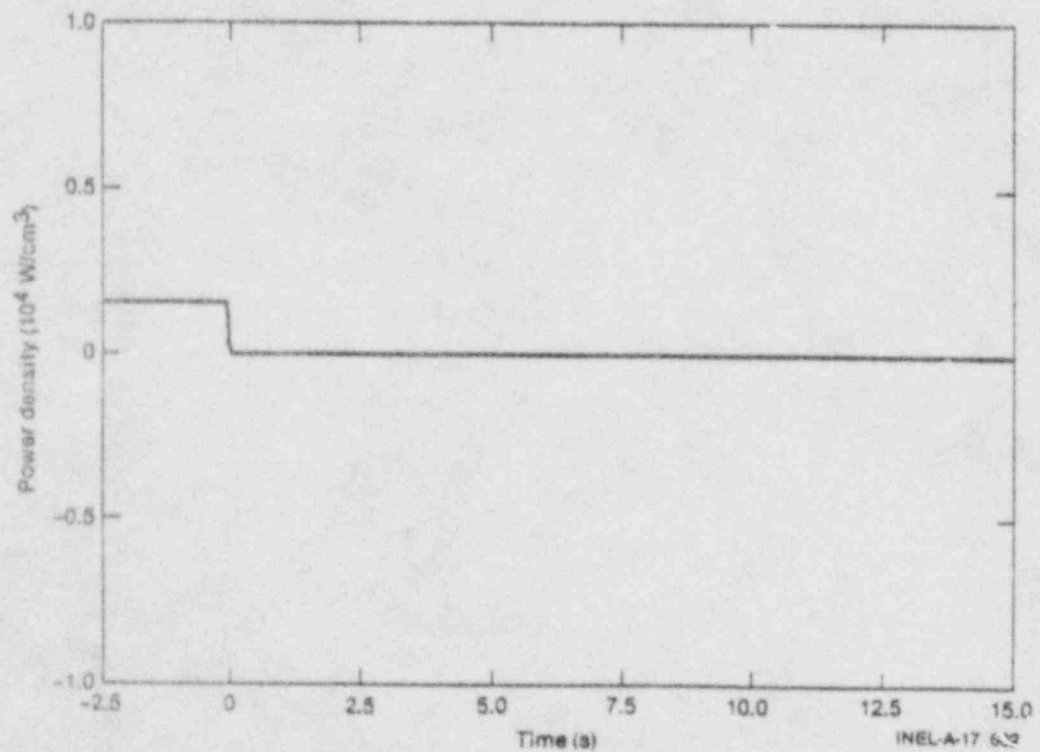
Fig. 18b. The Semiscale local rod power density function corresponding
to the electric rod data presented in Fig. 18a. The steady
state power is defined prior to t = 0.

50

Using the algorithm, the results of successive or iterative calcula-
tions have been made and are shown in Figures 19 thru 20. Figure 20a shows
that a good approximation is made on the third calculation and the result-
ing power function is displayed in Figure 20b. Notice that to match the
LOFT nuclear rod boundary conditions, the Semiscale rod must receive
negative power over two time periods during the length of the transient.
Both negative power requirements occur when the Semiscale rod is forced to
cool down like the nuclear rod.* Because of the negative power, it is not
realistically possible for the Semiscale heater rod to duplicate the
postulated nuclear rod surface boundary conditions as presented in
Figures 16 and 17. We shall continue to examine the cooldown behavior of
the Semiscale heater rod and a nuclear rod in the next section.

7.4 Comparison of RELAP Calculated and LTSF Measured Data

A series of rapid flooding tests were performed at the LOFT Test
Support Facility (LTSF) on a Semiscale heater rod. The principal objective
of the tests was to investigate the cooldown and quenching characteristics
of an electric heater rod with and without LOFT type surface cladding
thermocouples. The hydraulic conditions for the LTSF tests were selected
to approximate the rapid cooling transient that was observed during the
LOFT L2-3 LOCE. A review of the test data[7] clearly shows that the
exterior cladding thermocouple does quench sooner and much more rapidly
than the surface temperature of an uninstrumented rod. However, it is not
clear how these results can be applied to a nuclear rod since the Power
Burst Facility (PBF) TC-3 tests have indicated[8] that a nuclear rod is
capable of cooling down rapidly, much more rapidly than is expected for the
Semiscale heater rod based on the LTSF data.

---

* It has not yet been absolutely confirmed that the assumed nuclear rod
surface temperature quench actually occurred, or was simply a thermocouple
measurement phenomenon. However, several recent nuclear rod tests tend to
indicate that the LOFT cladding quench did occur and that it was not
greatly influenced by the surface cladding thermocouples.
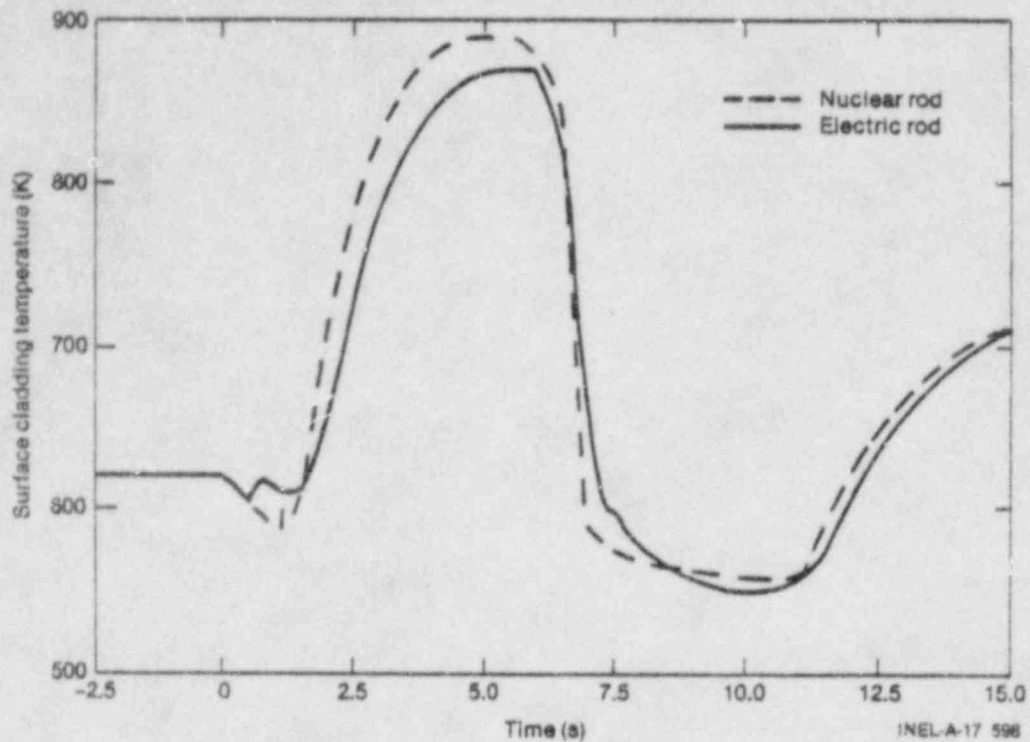
Fig. 19a. An overlay of the LOFT nuclear rod surface cladding temperature and the Semiscale temperature response assuming the local electric rod power density function defined in Fig. 19b, and the nuclear heat flux boundary condition described in Fig. 17. (Calculation 2)

Fig. 19b. The Semiscale local rod power density function as determined from the data presented in Fig. 18a, and used to produce the electric rod response shown in Fig. 19a.

Fig. 20a. An overlay of the LOFT nuclear rod surface cladding temperature
and the corresponding Semiscale temperature response assuming
the local electric rod power density function defined in Fig. 20b,
and the nuclear heat flux boundary condition described in Fig. 17.
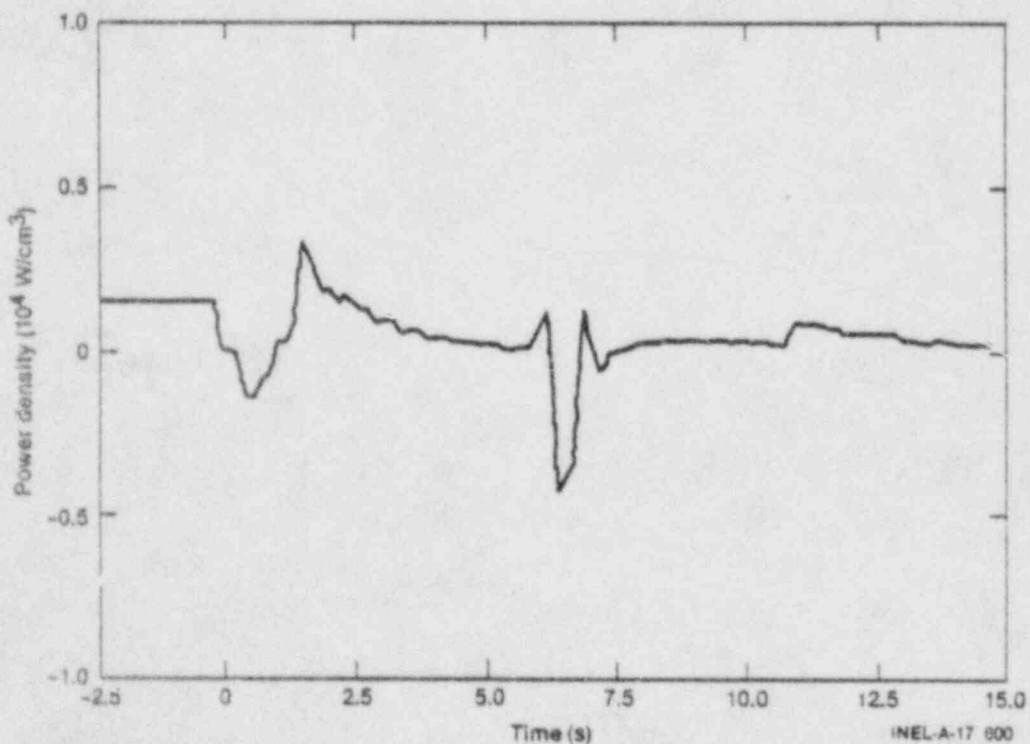(Calculation 3)

Fig. 20b. The Semiscale local rod power density function as determined
from the data presented in Fig. 19a, and used to produce the
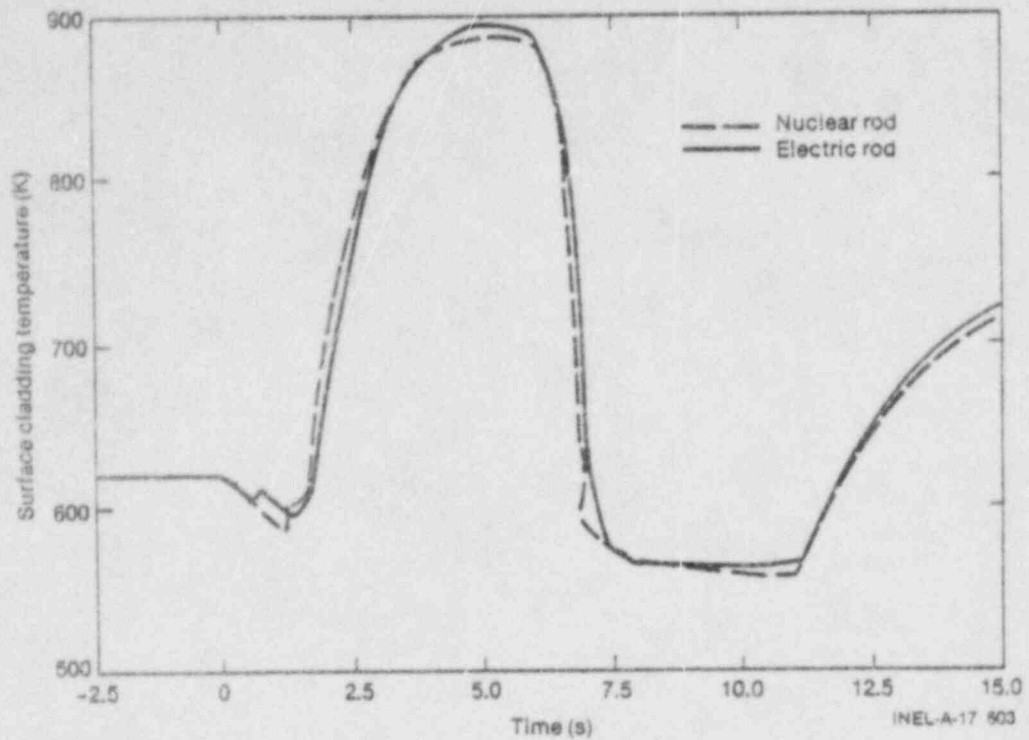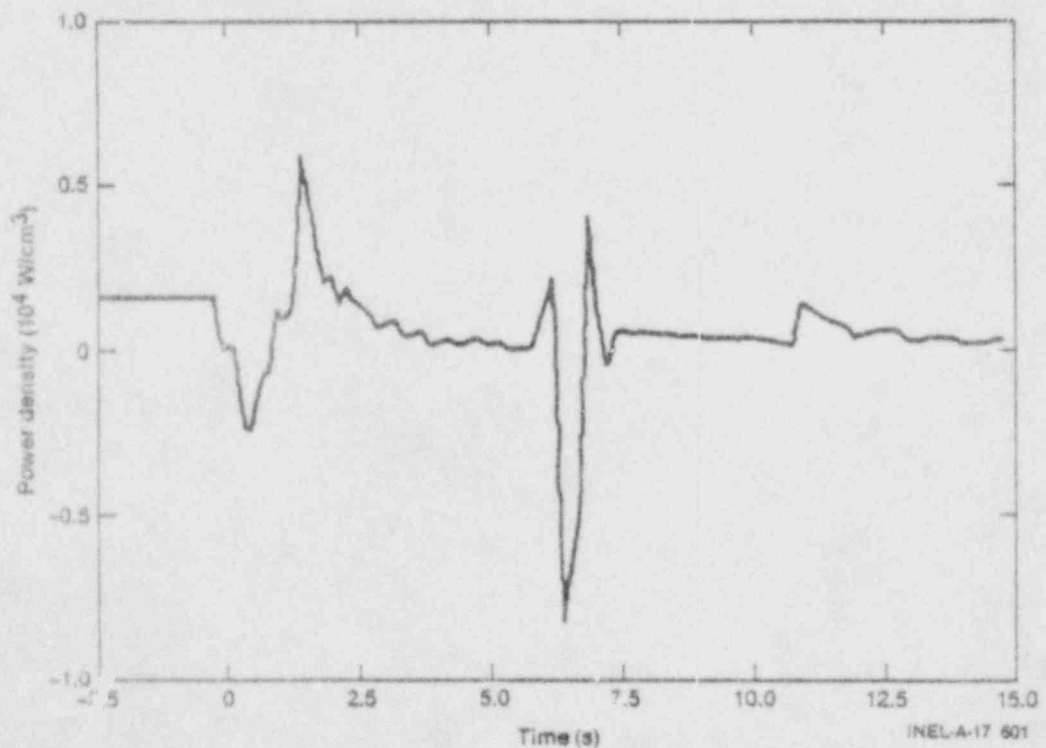electric rod response shown in Fig. 20a.

To better understand the reasons for the difference in responses of the electric and nuclear rods during rapid flooding events, a series of RELAP4/MOD6 calculations were undertaken. These computer code calculations centered on evaluating the response of a Semiscale heater rod and a nuclear rod under typical LTSF test conditions. The principal results of this work are shown in Figure 21.

In Figure 21, a best estimate RELAP4/MOD6 electric rod temperature response is compared with the measured LTSF electric rod data. The difference between the calculated and measured electric rod data is thought to be attributable to inaccurate modeling of the transition boiling regime by the code.

Figure 21 also illustrates the results of substituting a nuclear rod for the Semiscale electric rod and performing the same RELAP calculation. Clearly, the nuclear rod cladding is cooling down to the saturation temperature more rapidly than the electric rod. This discrepancy in rod behavior cannot be accounted for by making realistic changes in the electric rod input power. In fact, Figure 22 shows the required electric rod power necessary to simultaneously duplicate the nuclear rod surface temperature and surface heat flux as shown in Figures 21 and 23, respectively. Notice the large negative powers needed to force the electric rod to duplicate the nuclear rod response. Finally, Figure 24 shows an overlay of the nuclear and electric rod surfaces cladding temperatures where the Semiscale heater rod power function is defined in Figure 22.

The presence of unrealistic negative powers in the ideal electric rod powering function, which duplicates the nuclear rod boundary conditions, indicates that the observed differences in the electric and nuclear rod responses are the result of inherent limitations in the Semiscale rod design. Supporting analysis has shown that the primary items responsible for the problem are the thermal conductivity or thermal diffusivity of the insulator (BN vs. UO_2), and the absence of a thermal gas gap in the electric rod.
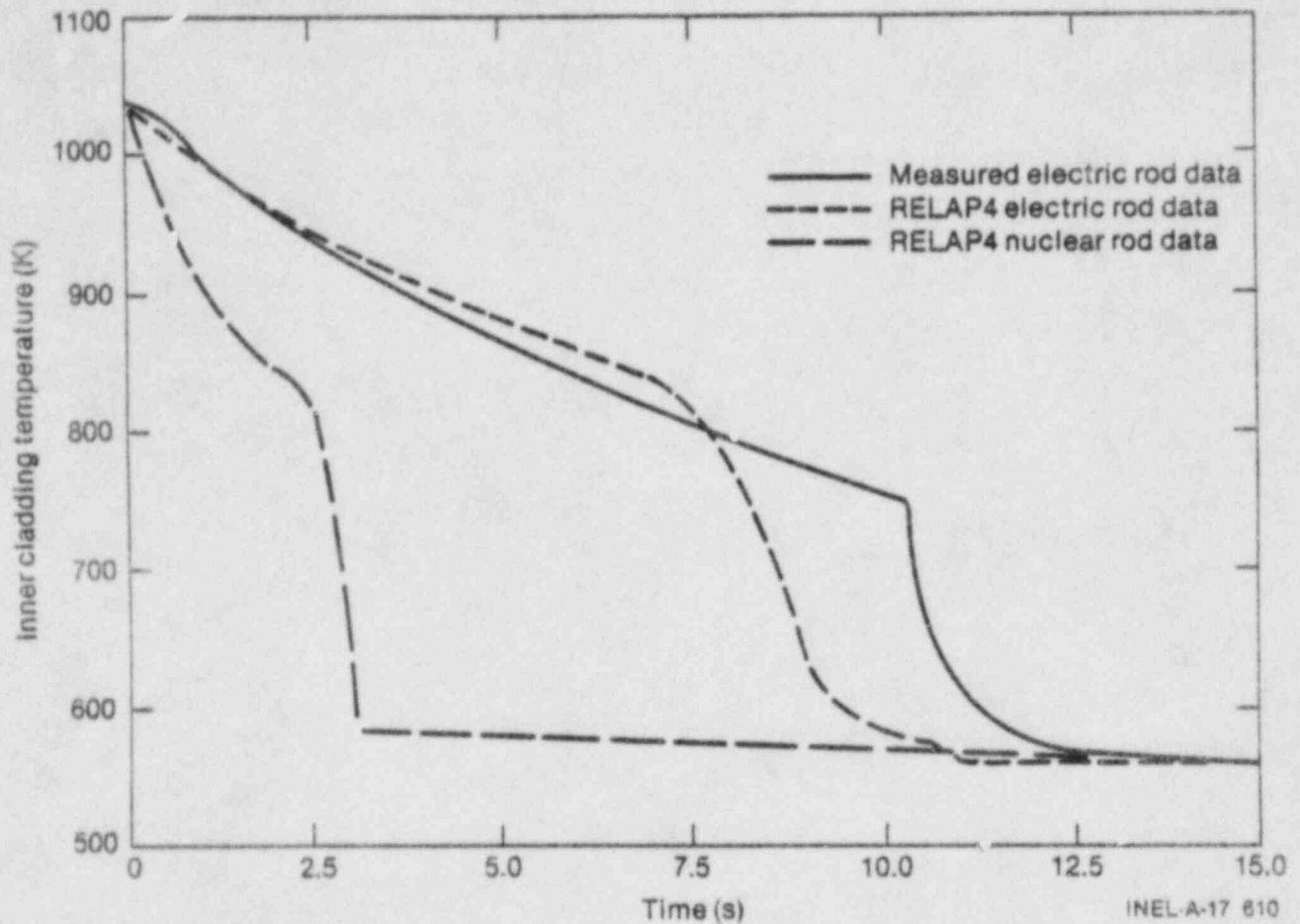
Fig. 21. An overlay of the measured and RELAP4 calculated electric and nuclear rod data, assuming LTSF quench test 12 thermal-hydraulic conditions. Notice that the calculated response of the nuclear rod indicates that the nuclear rod cools down more rapidly than either the measured or calculated electric rod response for the Semiscale heater rod.

55
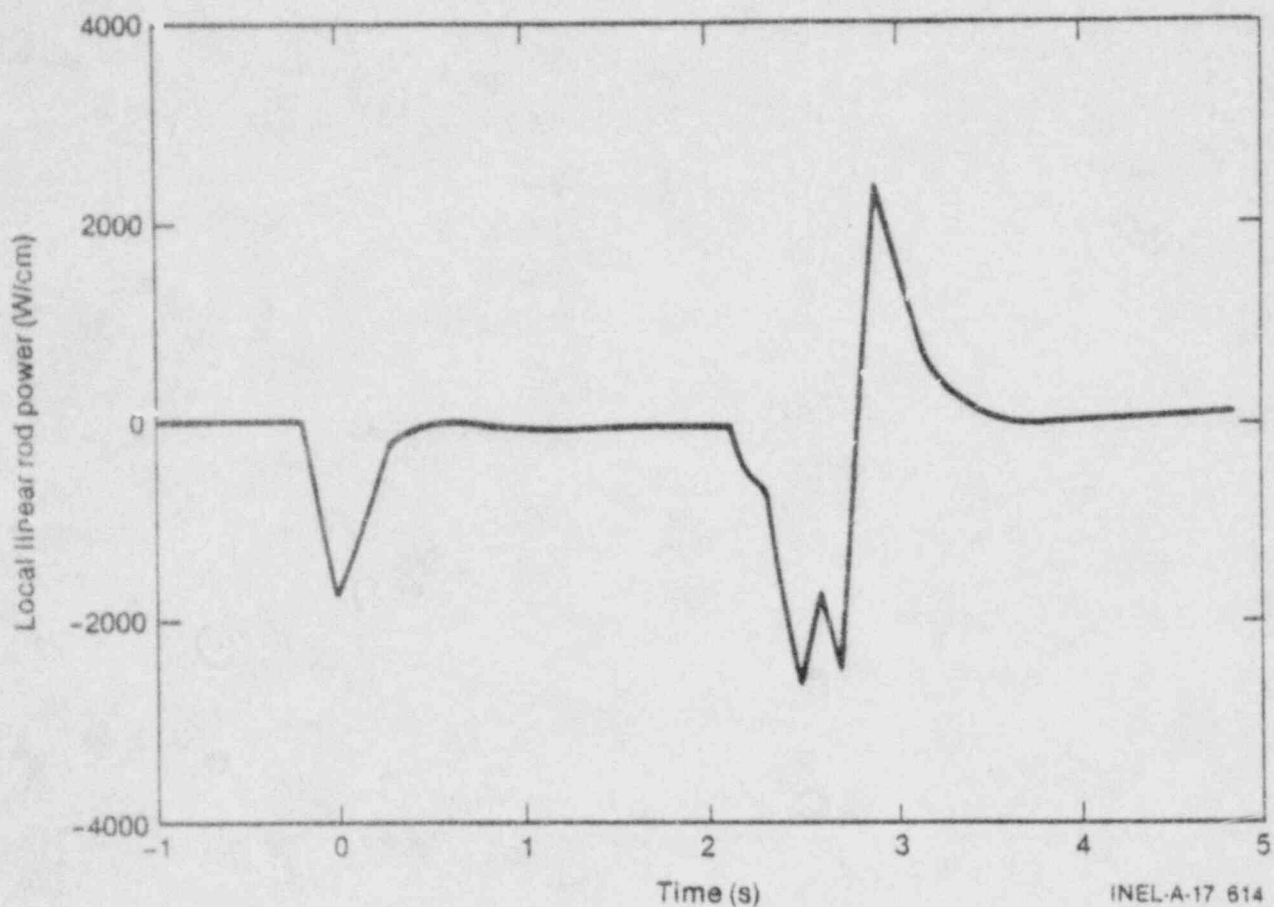
Fig. 22. The calculated Semiscale peak linear rod power needed to
duplicate the nuclear rod temperature response shown in
Fig. 21, assuming the nuclear heat flux boundary condition
shown in Fig. 23. Notice the large negative rod powers
needed to reproduce the nuclear rod response.
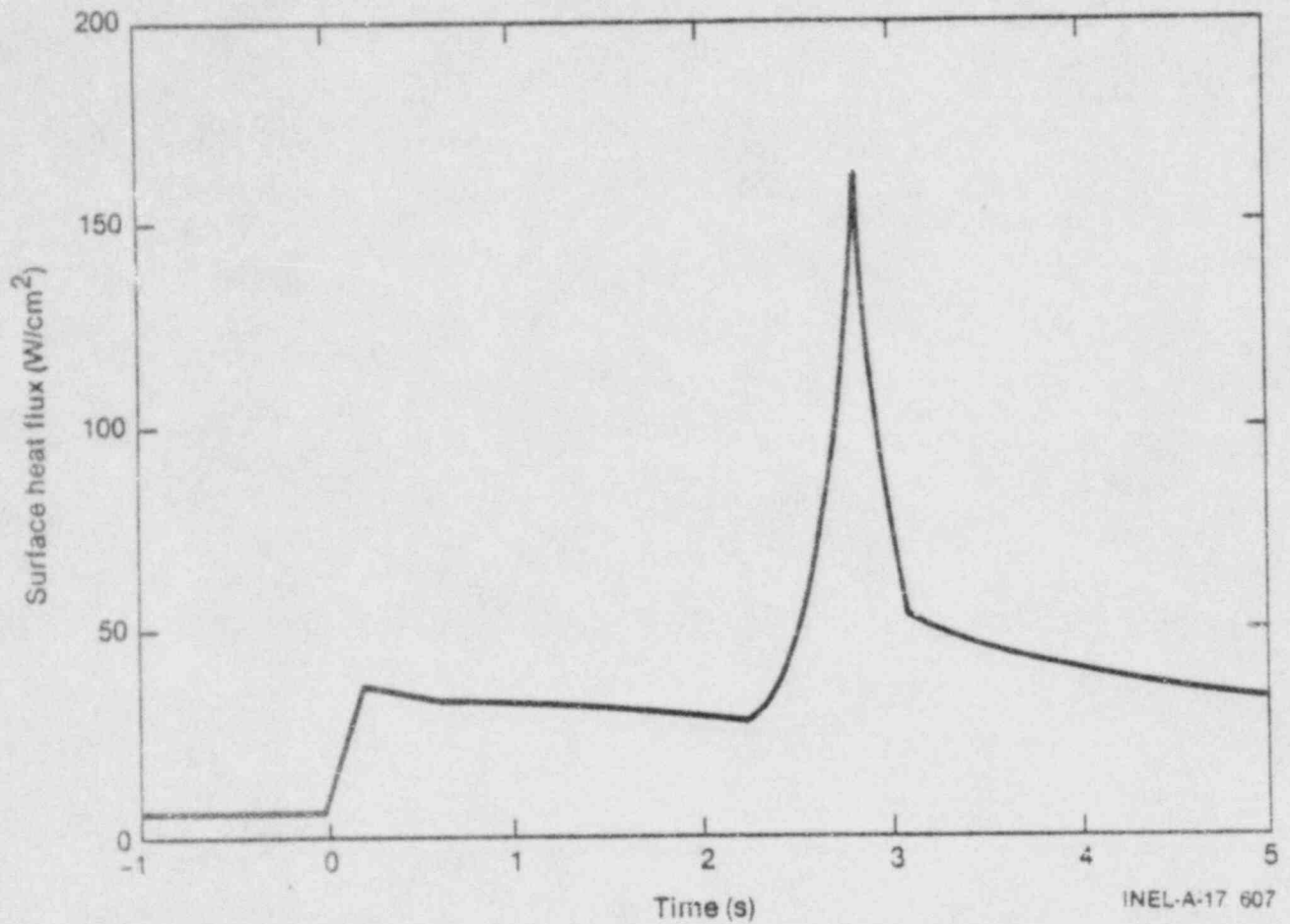
Fig. 23. The RELAP4 calculated nuclear surface heat flux corresponding to the nuclear surface temperature condition shown in Fig. 21.
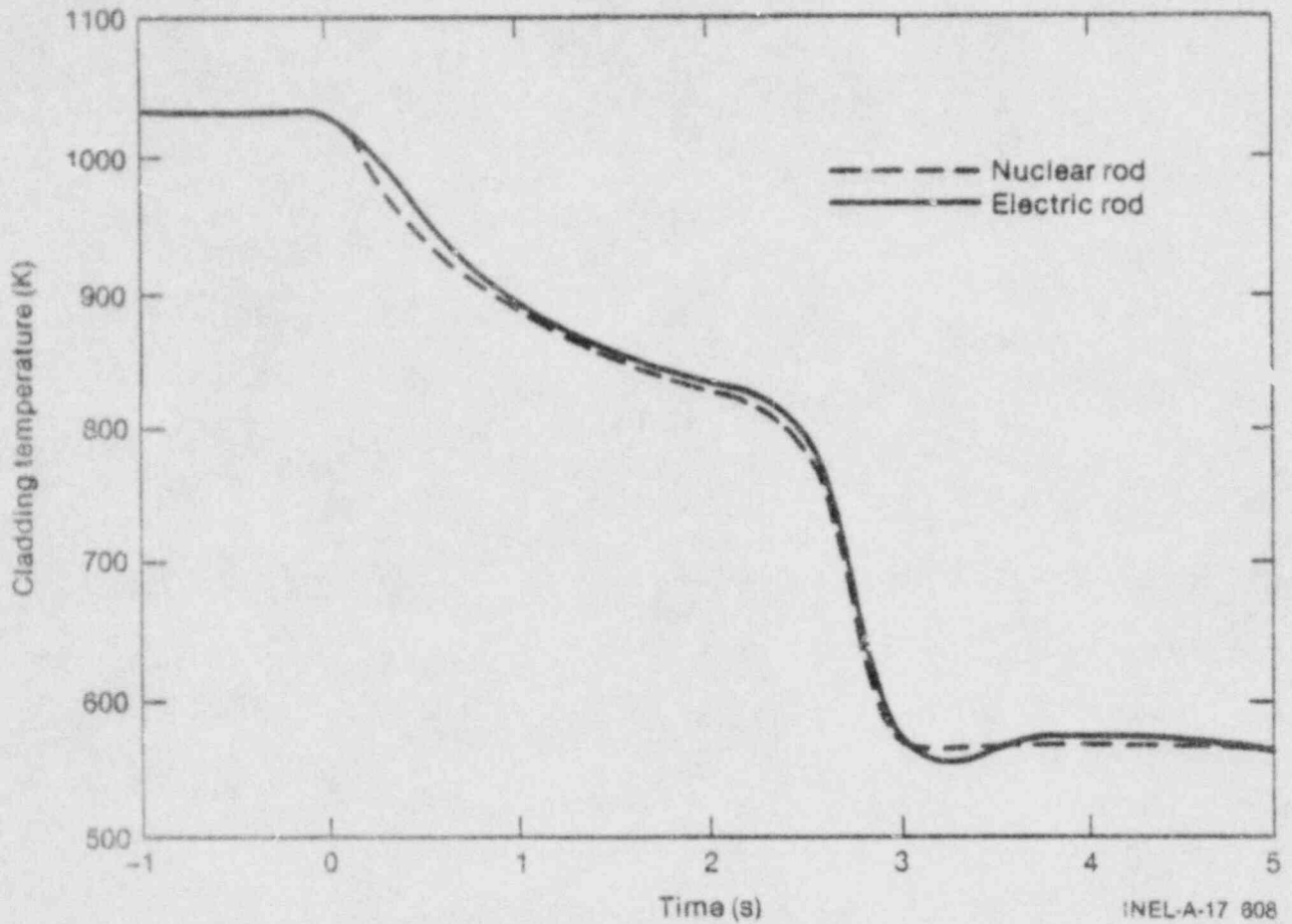
Fig. 24. An overlay of the RELAP4 calculated nuclear and Semiscale electric rod temperature responses, where the Semiscale rod power function is defined in Fig. 22.

Because of the low thermal conductivity of UO_2, the presence of cracks in the fuel, and the existence of a gap between the fuel and the cladding, the cladding of a nuclear rod is thermally decoupled from the stored energy and heat generation within the UO_2 pellet during rapid cooling transients. This is partly illustrated in Figure 25 by comparing the steady state nuclear and electric rod radial temperature profiles at rod powers of 39.4 kW/m (12 kW/ft). Here, the electric rod cladding is directly coupled to the inner heat source via the relatively low thermal resistance path provided by the BN insulation. This is evident in Figure 25 by noting the low temperature gradients that can be supported across the electric rod in contrast to the nuclear rod. Consequently, in order for the electric rod to cool down and quench, a much more uniform change and subsequently a larger fraction of the initial electric rod stored energy must be transported to the coolant than is necessary for the nuclear rod. This leads to the observed longer cooldown period for the electric rod relative to the nuclear rod, and therefore the inherent conservatism of the electric rod data with regard to estimating nuclear rod behavior during rapid cooling transients.

Fig. 25. An overlay of the Semiscale and nuclear rod steady state radial temperatures for a maximum linear rod power of 39.4 kW/m (12 kW/ft). The steepness of the nuclear rod temperature profile indicates a low coupling path between the cladding and the fuel. In contrast, the relative flat distribution in the electric rod shows a high degree of coupling between the inner heat source and the cladding.

60

8. CONCLUSIONS

Present experimental and theoretical data indicates that there exist rapid cooling transients for which the cooldown characteristics of a nuclear rod cannot be simulated with a Semiscal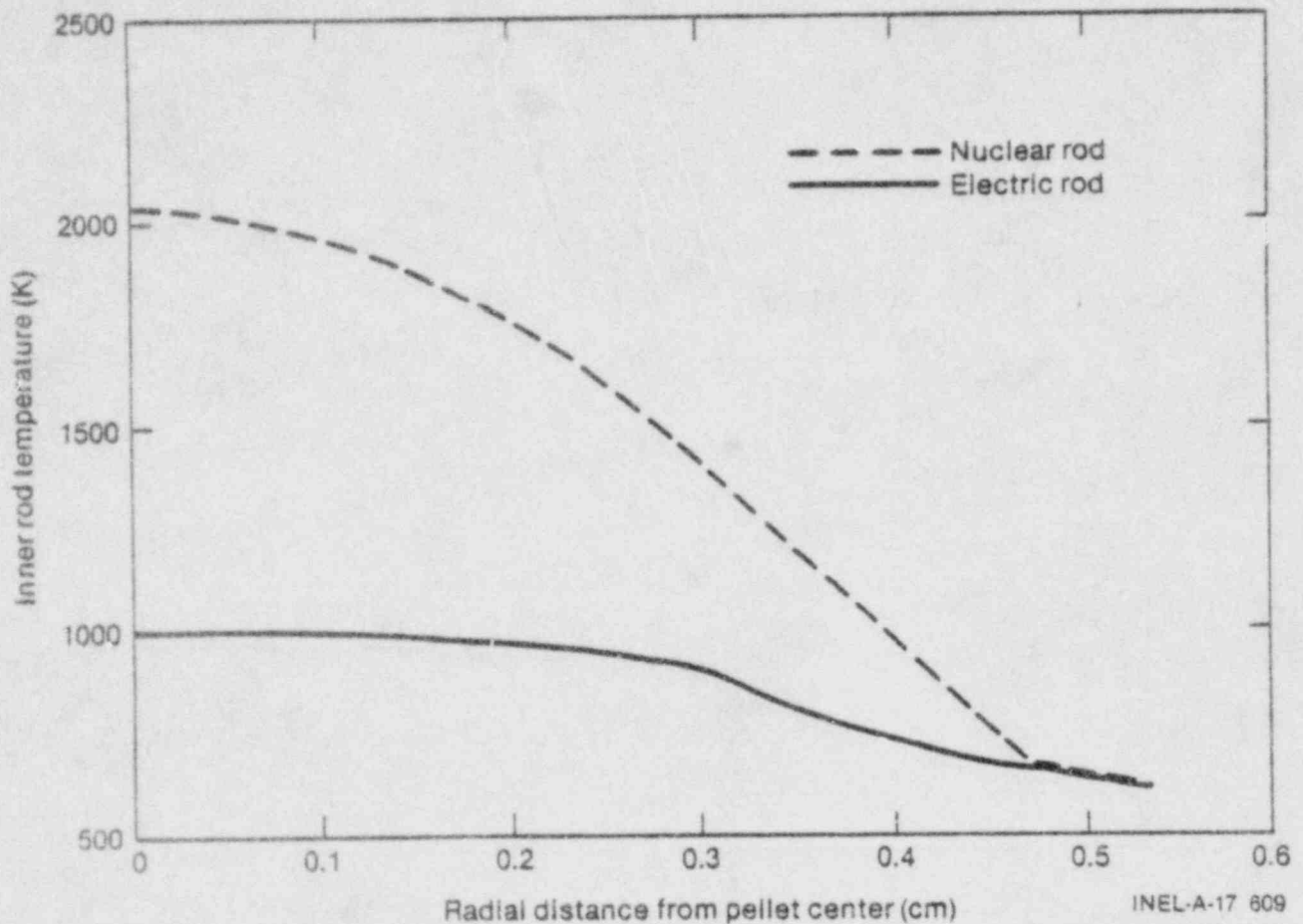e type heater rod under any sort of positive rod input powering scheme.* In other words, for certain rapid cooling events it appears that the Semiscale heater rod cannot cool down as quickly as a nuclear rod when both rods experience the same surface heat flux boundary condition, or the same heat transfer coefficient. This observation does not preclude the possibility that the Semiscale heater rod cannot experience a rapid cooldown event;** however, to do so the heat transfer coefficient (or surface heat flux) would have to be initially larger for the electric rod than is necessary for the nuclear rod.

The electric/nuclear rod simulation problem occurs during rapid cooling events because the nuclear rod cladding and the fuel heat source are partly decoupled via the existance of a clad-pellet gas gap and the low thermal conductivity of UO_2. This allows the nuclear rod cladding to cool down and quench as soon as the stored energy in the cladding is removed. For the solid type electric rod, however, the cladding and the internal heat source are directly coupled via a high thermal conductivity path provided by the thermal insulation and the non-existence of a gas gap. Consequently, a larger amount of rod energy must be removed from the electric rod before it can rewet. This phenomenon occurs even though the initial stored energy in the electric rod is less than the total stored energy in the nuclear rod.

---

* Assuming that both rods experience the same initial surface boundary conditions and the same transient hydraulic event.

** Note the Semiscale test data, Reference 9.

61

If significant thermal-hydraulic feedback exists between the surface heat transfer of a rod and its surrounding coolant, then the response of an electric rod may or may not be applicable to a nuclear rod under similar conditions. In fact, the ability of predicting key nuclear rod thermal-hydraulic phenomena from electric rod data is jeopardized whenever the response of the electric rod is sensitive to the rod input power function, which is in theory dependent upon unknown or uncertain nuclear rod boundary conditions. Resulting in a classical "bootstrap problem."

Even when the "ideal" electric rod power function is known, it might not be realistically possible to produce, e.g., negative rod powers. In any case, there are an infinite number of ways of powering an electric rod and they are all essentially incorrect except for at most one power function, which not only depends upon the same nuclear rod boundary conditions that are being estimated via the electric rod test, but may in fact turn out to be physically impossible to generate in the first place. Consequently, compromises are made in the electric rod input power function that make it difficult to interpret and understand the test results with regard to other electric rod test data and subsequent nuclear rod tests. These problems help to illustrate why it is so difficult, if not sometimes impossible, to simulate nuclear rod behavior with an electric rod; and further, to understand the implications of this data.

By comparing the theory of solid type internally heated rods and surface heated (direct) electric rods it is easy to believe that from a theoretical stand point the Zaloudek type heater rod might be superior to the solid type internally heated electric rods in simulation capability. At least it can be mathematically demonstrated that the Zaloudek heater rod can be realistically powered in such a way as to reproduce nuclear rod behavior. In comparison, solid type (indirect) heater rods of high internal thermal diffusivity cannot accomplish this criteria in all cases. Nevertheless, there do appear to be some engineering problems with the Zaloudek type rod that detract from its theoretical advantage over the

solid type rods. In particular, the three criteria assumed for the
Zaloudek rod cannot be exactly satisfied for a real rod. Also, theory
indicates that some of the problems associated with the solid type heater
rods can be alleviated by designing the rods with thermal insulation
material that more closely approximates the properties of UO_2. Finally,
one particular type of rod design that was not studied in the report, but
appears to hold much promise in simulating a nuclear rod, is the cartridge
type heater rod. The cartridge type rod is designed with a gas gap between
the cladding and the internal heat source, making it possible for the rod
to better simulate the nuclear heat delivery rate to the cladding.

REFERENCES

1. M. N. Ozisik, Boundary Valve Problems of Heat Conduction, International Textbook Company, 1968, Chapters 1 and 3.

2. R. V. Churchill, Fourier Series and Boundary Valve Problems, McGraw-Hill Book Company, 1941, Chapter 7.

3. T. Myint-U, Partial Differential Equations of Mathematical Physics, North Holland Scientific Publishers Ltd., 1980, pg. 145-148.

4. J. P. Dougherty and R. J. Muzzy, BWR 8x8 Fuel Rod Simulation Using Electrical Heaters, GEAP-21207, March 1976, Appendix A.

5. H. Stadtke, L. Piplies, Performance of Directly Heated Rods As Nuclear Rod Simulators in the LOBI Facility, A Paper presented at the 1980 Fuel Rod Simulator Symposium at Gatlinburg, TN. (Authors are affiliated with EURATOM--Joint Research Center at Ispra, Italy.)

6. Guide to the HEATO Code, SEMI-TR-003, March 1979.

7. R. C. Gottula, J. A. Good, The Effect of Cladding Surface Thermocouples on the Quench Behavior of an Electrical Heater Rod, LO-00-80-115, March 5, 1980.

8. T. R. Yackle, M. E. Waterman, P. E. MacDonald, Loss-of-Coolant Accident Test Series Test TC-1 Test Results Report, EGG-TFBP-5068, May 1980.

9. Quick Look Report for Semiscale MOD-1 Test S J6-3 LOFT Counterpart Test Series (Regulatory Standard Problem 8), WR-S-78-007, May 1978, Figure 16.

APPENDIX A

AN ANALYTICAL SOLUTION OF THE
LINEAR HEAT CONDUCTION DIFFERENTIAL EQUATION
SUBJECT TO TWO SIMULTANEOUS SURFACE BOUNDARY CONDITIONS

APPENDIX A

AN ANALYTICAL SOLUTION OF THE
LINEAR HEAT CONDUCTION DIFFERENTIAL EQUATION
SUBJECT TO TWO SIMULTANEOUS SURFACE BOUNDARY CONDITIONS

As we have already seen it is numerically possible, utilizing the HEATO conduction code in an interactive procedure, to evaluate a rod power function that will approximate the solution of the heat conduction differential equation subject to two simultaneous surface boundary conditions, as initialized from a steady state temperature distribution. It is the intent of this appendix to illustrate how an analytical solution can be derived for annular and cylindrical geometries.

We shall assume that for each region under consideration, the thermal conductivity (k) and the volumetric specific heat ($\gamma = \rho C_p$) are constants. It is noted, however, that this assumption is not particularly critical in the following analysis but it does facilitate solution of the problem.*

(Case 1)

We begin by writing the one-dimensional heat conduction differential equation in cylindrical coordinates:

$$\frac{\partial^2 T}{\partial r^2} + \frac{1}{r}\frac{\partial T}{\partial r} - \frac{1}{\alpha}\frac{\partial T}{\partial t} = \frac{-q'''}{k} \tag{A1}$$

---

* Although k and γ could be more generally treated as functions of the space variable r, it is still important that k and γ are not functions of temperature in order to preserve linearity of the heat conduction equation.

where,

T = $T(r,t)$ is the rod space time temperature function

α = k/γ is the rod material thermal diffusivity

k =   the rod thermal conductivity

γ = $\rho\, C_p$ = the rod volumetric specific heat

q''' =   the volumetric heat source.

The boundary conditions for (Al) are usually the rod surface temperature and surface heat flux. However, for the following analysis we shall assume that the rod surface temperature $[T_R = T(R,t)]$ and the rod surface temperature gradient

$$T_R' = \left.\frac{\partial T}{\partial r}\right|_{R,t}$$

are specified. In any case, knowledge of the rod surface temperature gradient and rod surface thermal conductivity implies knowledge of the rod surface heat flux $(\phi_R = \phi(R,t) = -kT_R')$. Also, the rod surface heat transfer coefficient $[h = \phi_R/(T_R - T_\infty)]$ can be determined if the bulk coolant temperature (T_∞) is known.

We now solve Equation (Al) for $T = T(r,t)$ when $T_R = T(R,t)$ and

$$T_R' = \left.\frac{\partial T}{\partial r}\right|_{R,t}$$

are specified functions of time t at surface $r = R$, and $q''' = 0$ between $r = R$ and $r = S$ where $R > S > 0$ as shown in Figure A1. We first assume tha the functions $T_R = T_R(t)$ and $T_R' = T_R'(t)$ can be represented by polynomials of finite degree $\leq m$ (where m is some non-negative integer) for the entire length of the transient. For instance,

$$T_R = T_R(t) = a_0 + a_1 t + a_2 t^2 + \ldots + a_m t^m \qquad \text{(A2-a)}$$

$$T_R' = T_R'(t) = b_0 + b_1 t + b_2 t^2 + \ldots + b_m t^m \qquad \text{(A2-b)}$$

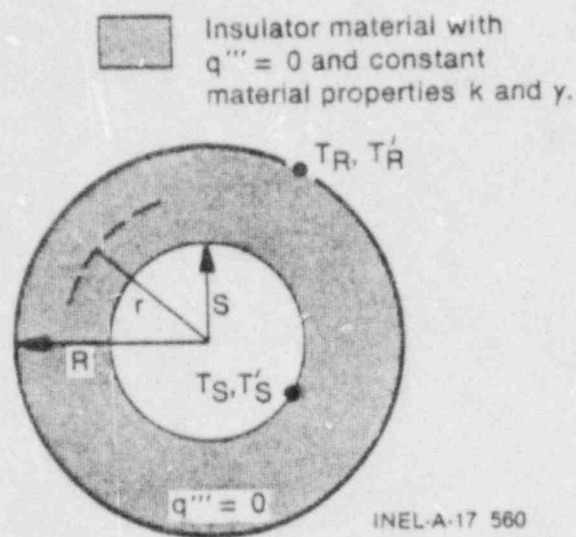where some or all of the coefficients a_i and b_i may be zero.

Fig. A1. An annular region of outer radius R and inner radius S, and no heat generation. Functions $T_R(t)$ and $T_R'(t)$ are specified at $r = R$ and material properties k and γ are assumed to be constant. Based on these assumptions, $T(r,t)$ and $T'(r,t)$ are calculated at $r = S$.

68

These equations are assumed to be valid for at least the transient $t > 0$ where $t \leq 0$ represents the time at which the rod is in a thermal steady state condition. The reason for the above assumptions for T_R and T_R' will be explained shortly, however, it might first be observed that these assumptions are not unreasonable since T_R and T_R' can always be approximated to within any degree of accuracy by polynomials. Further, such approximations are best suited for estimating the time derivatives of T_R and T_R' when both T_R and T_R' are defined by numerical data.

If T_R and T_R' are represented by polynomials of degree $\leq m$, then it follows that the $m + 1^{st}$ and all higher order time derivatives of T_R and T_R' are zero. That is,

$$\frac{\partial^{n+1} T_R}{\partial t^{n+1}} = 0 \qquad \text{where } n \geq m \tag{A3-a}$$

$$\frac{\partial^{n+1} T_R'}{\partial t^{n+1}} = 0 \qquad \text{where } n \geq m \tag{A3-b}$$

Now we assume that the solution of Equation (A1) takes the following series form:

$$T = T(r,t) = T_R + A(r) \, T_R' + B(r) \, \dot{T}_R + C(r) \, \dot{T}_R' + D(r) \, \ddot{T}_R + \ldots \tag{A4}$$

where the boundary conditions for T_R and T_R' require that

$$A(R) = B(R) = C(R) = D(R) = \ldots = 0 \tag{A5}$$

$$A'(R) = 1 \tag{A6}$$

$$B'(R) = C'(R) = D'(R) = \ldots = 0 \tag{A7}$$

69

$$\dot{T}_R = \frac{\partial T_R}{\partial t}, \quad \dot{T}_R' = \frac{\partial T_R'}{\partial t} = \frac{\partial^2 T}{\partial t \, \partial r}, \text{ etc.} \tag{A8}$$

Notice that because of conditions (A5), (A6), and (A7),

$$T(R,t) = T_R(t)$$

$$T'(R,t) = T_R'(t)$$

The specified boundary conditions

The form of Equation (A4) can be deduced by writing $T(r,t)$ in a Taylor series expanded about the point $r = R$ and then using Equation (A1) to evaluate the spatial derivates of $T(r,t)$ at $r = R$. Doing this and collecting together the coefficient terms of T_R', $\dot{T}_R$, $\dot{T}_R'$, etc., will lead to Equation (A4). In any case, it is not important how Equation (A4) is deduced but rather that functions $A(r)$, $B(r)$, $C(r)$, etc., can be determined so that (A4) is the desired solution of (A1) satisfying the two surface boundary conditions.

We further point out that at $t = 0$, considered the time at which the initial temperature distribution is specified, e.g., $T(r,0)$, Equation (A4) uniquely determines $T(r,0)$ once T_R and T_R' are specified and $A(r)$, $B(r)$, $C(r)$, etc. are computed. Therefore, according to Equation (A4) we are not free to arbitrarily select the initial temperature distribution $T(r,0)$. This should not cause any problems since the temperature distribution resulting from (A4) during steady state conditions is the correct distribution that would naturally result. Therefore, we shall assume that the transient calculation $(t > 0)$ is initialized from a steady state condition existing for $t \leq 0$. We will not consider the problem for which the transient calculation is initialized by some prior transient or some other atypical initial temperature distribution.

70

Getting back to the original problem we must determine functions $A(r)$, $B(r)$, $C(r)$, etc., so that Equation (A4) satisfies the heat conduction Equation (A1) with $q''' = 0$. We have already noted that $T(r,t)$ defined by (A4) satisfies the surface boundary conditions $T_R(t)$ and $T_R'(t)$.

Using (A4) we determine that:

$$T'' = A''(r) \, T_R' + B''(r) \, \dot{T}_R + C''(r) \, \dot{T}_R' + D''(r) \, \ddot{T}_R + \ldots$$

$$\frac{T'}{r} = \frac{A'(r)}{r} \, T_R' + \frac{B'(r)}{r} \, \dot{T}_R + \frac{C'(r)}{r} \, \dot{T}_R' + \frac{D'(r)}{r} \, \ddot{T}_R + \ldots$$

$$-\frac{\dot{T}}{\alpha} = \qquad\qquad -\frac{1}{\alpha} \, \dot{T}_R - \frac{A(r)}{\alpha} \, \dot{T}_R' - \frac{B(r)}{\alpha} \, \ddot{T}_R + \ldots$$

In order that $T'' + T'/r - T/\alpha = 0$ for all values of r and t, we must have that:

$$A'' + \frac{A'}{r} = 0 \tag{A9-a}$$

$$B'' + \frac{B'}{r} = \frac{1}{\alpha} \tag{A9-b}$$

$$C'' + \frac{C'}{r} = \frac{A(r)}{\alpha} \tag{A9-c}$$

Solving the above equations subject to the boundary conditions defined by Equations (A5), (A6), and (A7) we find that:

71

$$A(r) = 2 \ln (r/R) \qquad \text{(A10-a)}$$

$$B(r) = \frac{r^2 - R^2}{4\alpha} - \frac{R^2 \ln (r/R)}{2\alpha} \qquad \text{(A10-b)}$$

$$C(r) = \frac{R r^2}{4\alpha} [\ln (r/R) - 1] + \frac{R^3}{4\alpha} [\ln (r/R) + 1] \qquad \text{(A10-c)}$$

Since the $(m+1)^{st}$ and higher order time derivates of T_R and T_R' are assumed to be zero,* then there are at most a finite number of non-zero terms in the (A4) series representation of $T(r,t)$, and therefore the series converges. Also, it can be shown that under the conditions considered for this problem the solution is unique. Therefore, Equation (A4) represents the solution of the heat conduction differential equation satisfying the two surface boundary conditions. It is not necessary to require that T_R and T_R' be represented by polynomials in order to establish convergence of the series (A4), but it is more diffi~~t to establish simple criteria that will guarantee such convergence for a more general case.

Using Equation (A4), estimates can be made for the temperature and temperature gradient at $r = S$; namely, $T_S = T(S,t)$ and

$$T_S' = \frac{\partial T}{\partial r}\bigg|_{S,t}.$$

---

* Since T_R and T_R' are approximated by polynomials.

Now we consider a uniformly heated solid cylinder of radius $r = S$ with surface boundary conditions T_S and $T_S{}'$.

(Case 2)

Assuming that the surface boundary conditions T_S and $T_S{}'$ are either specified or calculated via an application of (Case 1), we now determine a function $q'''(t)$ which represents a uniform power source term and a function $T(r,t)$ which satisfies Equation (A1) and agrees with the surface boundary conditions and produces a finite temperature or zero temperature gradient at $r = 0$, note Figure A2
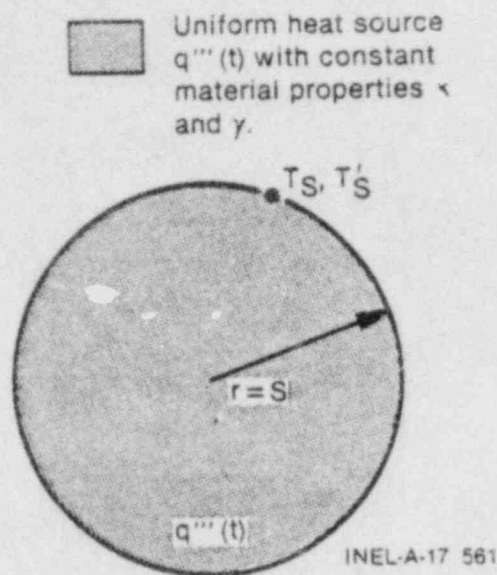

Fig. A2. A solid cylindrical rod of radius $r = S$ and uniform power source $q'''(t)$ with constant material properties k and γ. Surface boundary conditions T_S and T_S' are assumed to be specified.

Again we assume that $T(r,t)$ takes on the following series form:

$$T(r,t) = T_S + A(r)\, T_S' + B(r)\, \dot{T}_S + C(r)\, \dot{T}_S' + D(r)\, \ddot{T}_S + \ldots \tag{A11}$$

where the functions $A(r)$, $B(r)$, $C(r)$, etc., must be determined. We begin by writing the following equations:

$$T'' = A''(r)\, T_S' + B''(r)\, \dot{T}_S + C''(r)\, \dot{T}_S' + D''(r)\, \ddot{T}_S + \ldots$$

$$\frac{T'}{r} = \frac{A'(r)}{r}\, T_S' + \frac{B'(r)}{r}\, \dot{T}_S + \frac{C'(r)}{r}\, \dot{T}_S' + \frac{D'(r)}{r}\, \ddot{T}_S + \ldots$$

$$-\frac{\dot{T}}{\alpha} = \qquad\qquad -\frac{1}{\alpha}\dot{T}_S \; -\frac{A(r)}{\alpha}\, \dot{T}_S' \; -\frac{B(r)}{\alpha}\, \ddot{T}_S + \ldots$$

$$\rule{9cm}{0.4pt}$$

$$\frac{-q}{k} = a_o\, T_S' \; + \; b_o\, \dot{T}_S \; + \; c_o\, \dot{T}_S' \; + \; d_o\, \ddot{T}_S + \ldots$$

Here we have assumed a series expansion for $q'''(t)/k$ where a_o, b_o, c_o, etc., are as yet undetermined constants. In order that $T'' + T'/r - T/\alpha = -q'''/k$ for all values of r and t, we must have that

$$A''(r) + \frac{A'(r)}{r} = a_o \tag{A12-a}$$

$$B''(r) + \frac{B'(r)}{r} = \frac{1}{\alpha} + b_o \tag{A12-b}$$

$$C''(r) + \frac{C'(r)}{r} = \frac{A(r)}{\alpha} + c_o \tag{A12-c}$$

The new boundary conditions are:

$$A(S) = B(S) = C(S) = \ldots = 0 \tag{A13-a}$$

$$A'(S) = 1 \tag{A13-b}$$

$$B'(S) = C'(S) = \ldots = 0 \tag{A13-c}$$

$$A'(0) = B'(0) = C'(0) = \ldots = 0 \tag{A13-d}$$

Notice that condition (A13-d) is introduced so that the temperature gradient of $T(r,t)$ is zero at $r = 0$. The solutions of the equations in (A12) subject to the boundary conditions in (A13) are:

$$A(r) = \frac{r^2 - S^2}{2S} \quad \text{and} \quad a_0 = \frac{2}{S} \tag{A14-a}$$

$$B(r) = 0 \quad \text{and} \quad b_0 = \frac{-1}{\alpha} \tag{A14-b}$$

$$C(r) = \frac{1}{32 \alpha S} [r^4 - 2 S^2 r^2 + S^4] \quad \text{and} \quad c_0 = \frac{S}{4\alpha} \tag{A14-c}$$

$$D(r) = 0 \quad \text{and} \quad d_0 = 0 \tag{A14-d}$$

$$E(r) = \frac{1}{2304 \, \alpha^2 \, S} [2r^6 - 9S^2 r^4 + 12S^4 r^2 - 5S^6] \tag{A14-e}$$

$$\text{and} \quad e_0 = \frac{-S^3}{96 \, \alpha^2}$$

$$F(r) = 0 \quad \text{and} \quad f_0 = 0 \tag{A14-f}$$

$$G(r) = \frac{1}{73728 \; \alpha^3 \; S} \, [r^8 - 8S^2 \, r^6 + 24S^4 \, r^4 - 28S^6 \, r^2 + 11S^8]$$

$$\text{and } g_0 = \frac{1}{1536} \frac{S^5}{\alpha^3} \tag{A14-g}$$

$$H(r) = 0 \quad \text{and} \quad h_0 = 0 \tag{A14-h}$$

.
.
.

The functions $A(r)$, $B(r)$, $C(r)$, etc., uniquely determine the function $T(r,t)$ which satisfies the given boundary conditions and the heat conduction equation. Also, the numbers a_0, b_0, c_0, etc., determine the uniform power source term $-q'''/k$. Solving for q''' we write:

$$q''' = \frac{-2 \; k}{S} \; T_S' + \gamma \; \dot{T}_S - \frac{S \; k}{4\alpha} \; \dot{T}_S' + \frac{S^3}{96 \; \alpha^2} \; k \; \ddot{T}_S' + \ldots \tag{A15}$$

Notice the term

$$\gamma \; \dot{T}_S = \gamma \left. \frac{\partial T}{\partial t} \right|_{S,t}$$

in Equation (A15).

This term also appears as a term in Equation (29) for the hybrid calculation.

76

Since the surface heat flux $\phi_S(t) = \phi(S,t) = -kT_S'$, then q''' can also be written in the following form:

$$q'''(t) = \frac{2}{S}\phi_S + \gamma \dot{T}_S + \frac{S}{4\alpha}\dot{\phi}_S - \frac{S^3}{96\,\alpha^2}\ddot{\phi}_S + \ldots \tag{A16}$$

Equation (A16) is very similar to the formula presented in Equation (22) for the LOBI rod when $R_i = 0$ and $R_o = S$. The solutions for $T(r,t)$ and $q'''(t)$ are unique in that any two pair of solutions T_1, q_1''' and T_2, q_2''' which satisfy the same heat conduction differential equation, the same two surface boundary conditions, and the same initial temperature condition, necessarily implies that $T_1 = T_2$ and $q_1''' = q_2'''$. Therefore, the solution for q''', as shown in Equation (A16), proves that the time dependent rod power function necessary to duplicate the specified surface temperature and surface heat flux conditions is itself a function of these boundary conditions. Consequently, to properly power an electric rod to match the response of a nuclear rod, it is necessary that the nuclear surface boundary conditions be known. In addition, it is also necessary that the electric rod be subjected to the same nuclear hydraulic conditions.

There are several ways by which the above result can be extended. First, the results can be extended to cover annular heated regions instead of cylindrically heated geometries; and second, it can be extended to power distributions that are not uniform. For instance, if $q'''(r,t) = P(t)\,Q(r)$ where $Q(r)$ is some fixed radial power distribution and $P(t)$ is the time-dependent power factor. Further, by alternating between or patching together separate results one can also solve for complicated multifaceted rod geometries like that in Figure (A3).
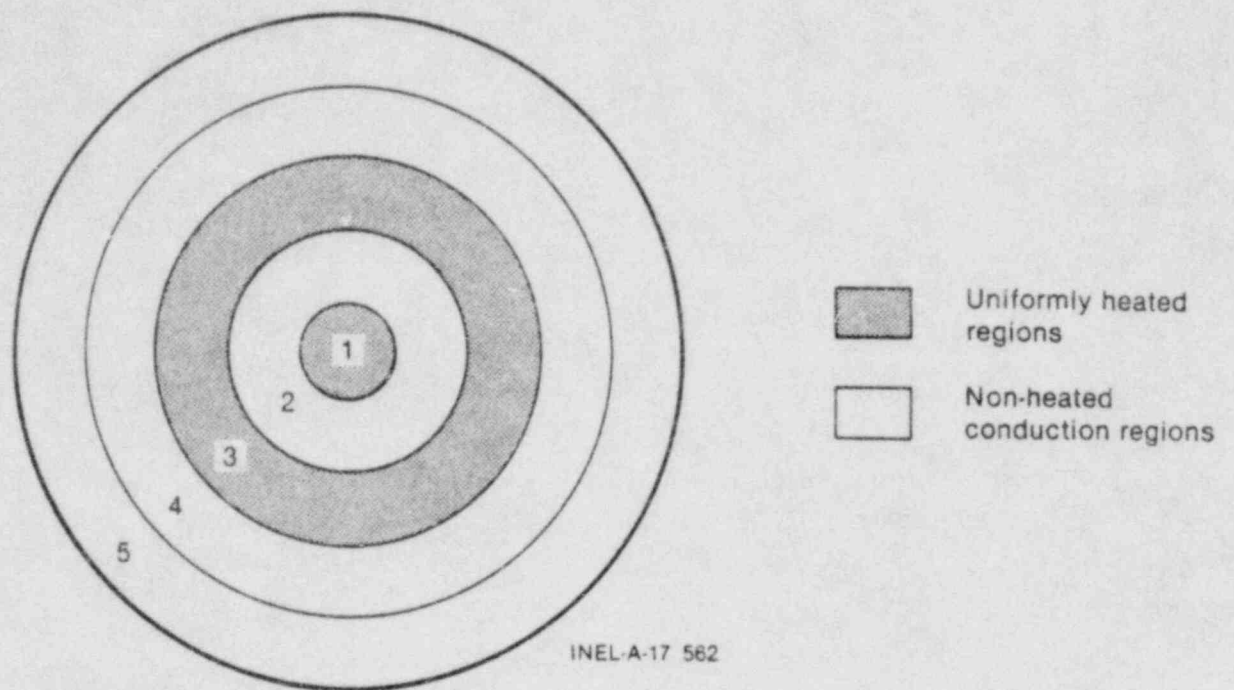
INEL-A-17 562

Fig. A3. An example of a complicated heater rod design with two separately powered but uniformly heated heater elements, and three non-powered conduction regions.

The end result of this analysis is that for many different heater rod geometries it is possible to derive a heater rod power function and a space-time temperature distribution function which solves the heat conduction differential equation and duplicates the prescribed boundary conditions. And not too surprisingly, the resultant power source function is dependent upon these surface boundary conditions.

APPENDIX B

TYPICAL HEATO INPUT DECKS

APPENDIX B

TYPICAL HEATO INPUT DECKS

Figure B1 illustrates the geometry, dimensions, and materials associated with the HEATO computer code models used to simulate the Semiscale heater rod. Figure B2 shows the general input used for the temperature independent HEATO calculations where the heater rod element has been modeled between the radial nodes 3 and 8. For a UDHS model one would simply place the heater element between nodes 1 and 20 (for this particular input deck); however, in order to initilize the algorithm to solve for the electric rod transient power it is not really necessary to start with the UDHS model. In fact, it might not even be necessary to begin with a temperature independent model of the Semiscale rod; nevertheless, this is usually done to avoid false temperature feedback effects in the initial estimate of $q_E'''(t)$. Finally, Figure B3 shows the input cards needed to run a HEATO model of the Semiscale heater rod with temperature dependent materials, resulting in temperature feedback effects. For this example, the rod surface heat flux boundary condition and the rod input power density are read from the attached data tape 21 with user supplied record numbers on lines 570 and 580.

When negative rod powers are the result of the hybrid calculations, then the significance of the temperature dependent HEATO model might be questioned. However, since negative rod powers are not possible for the Semiscale heater rod anyway, it is really immaterial "how" or "if" temperature feedback should be considered in the heater rod models in the first place.
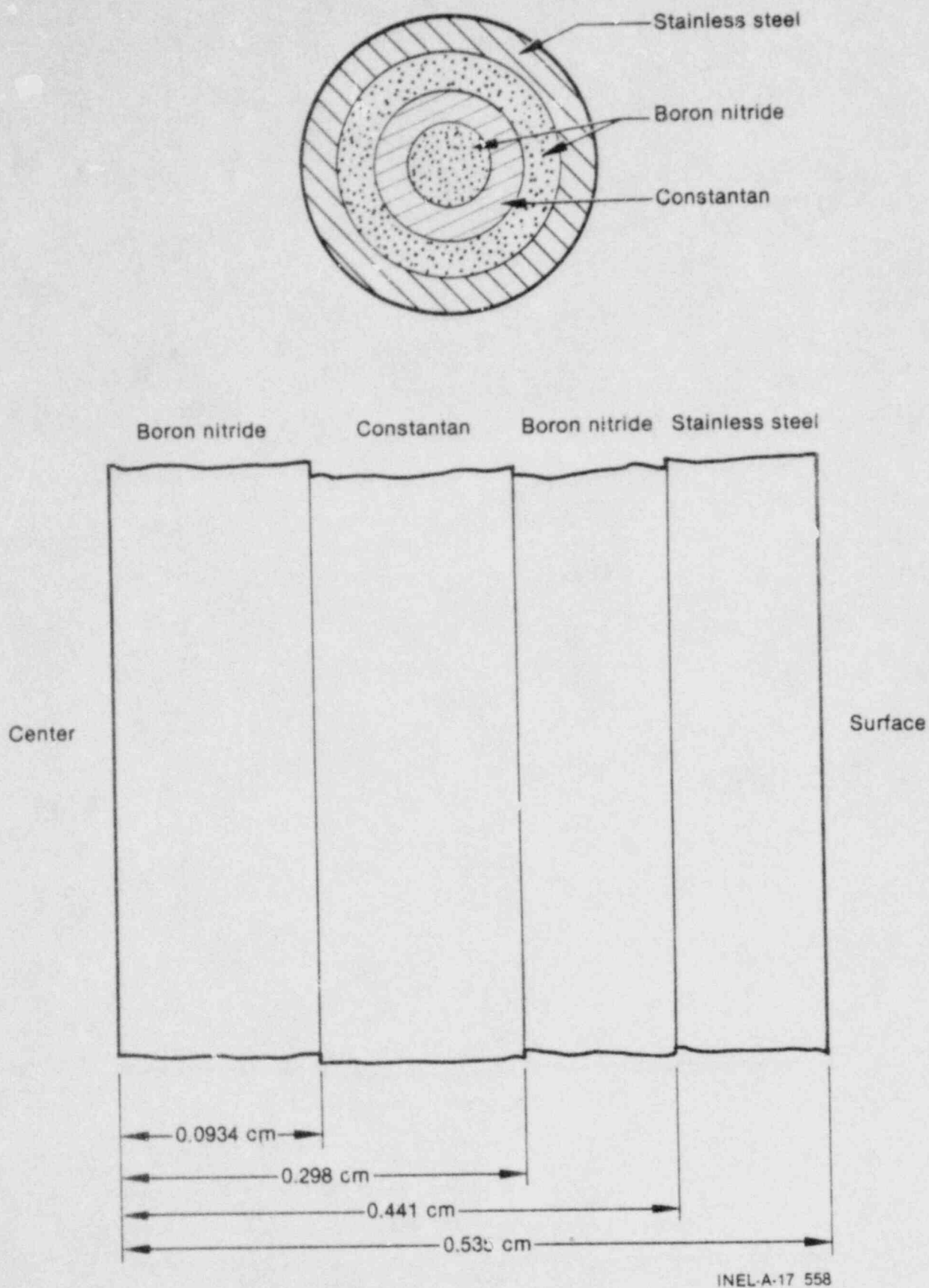
Fig. 81. A one-dimensional cylindrical model of the Semiscale MOD-1 heater rod.

82

```
100-UID,T37,P2.
110-ACCOUNT,SOURCE CODE,CHARGE NUMBER,BIN NUMBER.
120 ATTACH,ENVRL,ENVRL176D,ID-RJW.
130 TTACH,KXRLIB,ID-KXR,MR-1.
140-LIBRARY,ENVRL,KXRLIB.
150-ATTACH,TAPE21,INPUT-FILE-NAME,ID-UID,MR-1,CY-?.
160-REQUEST,TAPE8,*PF.
170-ATTACH,HEATOB,ID-DOS,MR-1.
180-HEATOB,PL-30000.
190-CATALOG,TAPE8,OUTPUT-FILE-NAME,ID-UID,MR-1,RP-999.
200-*EOR
210-PROP
220-K,1 INSIDE BN
230-0.0 0.10 5000.0 0.10
240-CP,1 INSIDE BN
250-0.0 3.74 5000.0 3.74
260-K,2  BN/CONSTANTAN MIX
270-0.0 0.24 5000. 0.24
280-CP,2 BN/CONSTANTAN MIX
290-0.0 3.8 5000. 3.8
300-K,3  OUTSIDE BN
310-0.0 0.13 5000. 0.13
320-CP,3 OUTSIDE BN
330-0.0 3.1 5000. 3.1
340-K,4 SS
350-0.0 0.18 5000. 0.18
360-CP,4 SS
370-0.0 4.3 5000. 4.3
380-END
390-MODEL
400--CONDUCTION MODEL #1
410-01010001 21 2 0.0 1.0 10 0.5 0
420-01010200 0 1

430-01010201 3 .09337 5 0.29837 5 0.44087 7 0.5348
440-01010301 1 3 2 8 3 13 4 20
450-01010401 0.0 3 1.0 8 0.0 20
460-01010601 620. 21
470-/
480-BCL,2,0.0
490-TIME,-10.0,15.0,0.05
500-BCR,2, TAPE CWAF 21 RECORD-NUMBER
510-POWER, -10.0,1561.7 -0.1,1561.7 0.0,0.0 15.0,0.0
520-START,1,50,0.01,STEADY
530-*EOR
540-*EOF
```

Fig. B2. A temperature independent Semiscale heater rod model
input deck for HEATO.

```
100-UID,T37,P2.
110-ACCOUNT,SOURCE CODE,CHARGE NUMBER,BIN NUMBER.
120-ATTACH,ENVRL,ENVRL176D,ID=RJW.
130-ATTACH,KXRLIB,ID=KXR,MR=1.
140-LIBRARY,ENVRL,KXRLIB.
150-ATTACH,TAPE21,INPUT-FILE-NAME,ID=UID,MR=1,CY=?.
160-REQUEST,TAPE8,*PF.
170-ATTACH,HEATOB,ID=DOS,MR=1.
180-HEATOB,PL=30000.
190-CATALOG,TAPE8,OUTPUT-FILE-NAME,ID=UID,MR=1,RP=999.
200-*EOR
210-PROP
220-K,1       BN THERMAL CONDUCTIVITY (W/CM K)
230-311.,0.16, 533.,0.14, 755.,0.115, 922.,0.10, 1099.,0.085
240-1255.,0.065, 1339.,0.06, 1600.,0.05
250-CP,1      BN VOLUMETRIC HEAT CAPACITY (J/CM3 K) DENSITY=2.01G/CM3
260-311.,1.79, 533.,2.73, 755.,3.36, 922.,3.74, 1099,4.02
270-1255.,4.30, 1422.,4.58, 1600.,4.90
280-K,2       CONSTANTAN THERMAL CONDUCTIVITY (W/CM K)
290-400.,0.217, 600.,0.297, 800.,0.378, 1000.,0.459, 1200.,0.540
300-1400.,0.621, 1600.,0.701
310-CP,2      CONSTANTAN VOLUMETRIC HEAT CAPACITY (J/CM3 K) DEN=8.92
320-400.,3.82, 600.,4.09, 800.,4.37, 1000.,4.64, 1200.,4.91
330-1400.,5.19, 1600.,5.46
340-K,3       SS-316 THERMAL CONDUCTIVITY (W/CM K)
350-400.,0.150, 600.,0.176, 800.,0.203, 1000.,0.230, 1200.,0.257
360-1400.,0.284
370-CP,3      SS-316 VOLUMETRIC HEAT CAPACITY (J/CM3 K) DEN=8.06/CM3
380-400.,4.0, 600.,4.28, 800.,4.55, 1000.,4.83, 1200.,5.10, 1400.,5.4
390-K,4       BN/CONSTANTAN MIX (50/50)    (W/CM K)
400-311.,0.17, 533.,0.205, 755.,0.238, 922.,0.264, 1099.,0.29
410-1255.,0.314, 1339.,0.328, 1600.,0.38
420-CP,4      BN/CONSTANTAN MIX (50/50)   (J/CM3 K)

430-311.,2.74, 533.,3.36, 755.,3.83, 922.,3.74, 1099.,4.39
440-1255.,4.64, 1422.,4.9, 1600.,5.18
450-END
460-MODEL
470--CONDUCTION MODEL #1
480-01010001 21 2 0.0 1.0 10 0.5 0
490-01010200 0 1
500-01010201 3 .09337 5 0.29837 5 0.44087 7 0.5348
510-01010301 1 3 4 8 1 13 3 20
520-01010401 0.9 3 1.0 8 0.0 20
530-01010601 620. 21
540-/
550-BCL,2,0.0
560-TIME,-10.0,15.0,0.05
570-BCR,2, TAPE CHAF 21 RECORD-NUMBER
580-POWER, TAPE CHAF 21 RECORD-NUMBER
590-START,1,50,0.01,STEADY
600-*EOR
610-*EOF
```

Fig. B3. A standard (temperature dependent) Semiscale heater rod
          model input deck for HEATO.

APPENDIX C

DEFINITIONS OF ACRONYMS AND INITIALISMS USED IN THE REPORT

APPENDIX C

DEFINITIONS OF ACRONYMS AND INITIALISMS USED IN THE REPORT

Abbreviation	Definition
BC	Boundary condition
DE	Differential equation
DNB	Departure from nucleate boiling
IC	Initial condition
IR	Inside radius
LOBI	Loop Blowdown Investigations (Facility)
LOFT	Loss-of-Fluid Test (Facility)
LOCE	Loss-of-coolant experiment
LTSF	LOFT Test Support Facility
PBF	Power Burst Facility
OR	Outside radius
UDHS	Uniformly distributed heat source